

Surface activity distribution measurements and establishment of a dose rate map inside the destroyed Chernobyl reactor

Chesnokov, A.V.; Fedin, V.I.; Gulyaev, A.A.; Potapov, V.N.; Shcherbak, S.B.; Smirnov, S.V.; Urutskoev, L.I.; Volkovich, A.G.; Shcherbin, V.N.; Gerasko, V.N.; Korneev, A.A.; Würz, H.; Fogh, C.L.; Andersson, Kasper Grann; Roed, Jørn

Publication date:
1999

Document Version
Publisher's PDF, also known as Version of record

[Link back to DTU Orbit](#)

Citation (APA):
Chesnokov, A. V., Fedin, V. I., Gulyaev, A. A., Potapov, V. N., Shcherbak, S. B., Smirnov, S. V., ... Roed, J. (1999). Surface activity distribution measurements and establishment of a dose rate map inside the destroyed Chernobyl reactor. (Denmark. Forskningscenter Risoe. Risoe-R; No. 1074(EN)).

DTU Library

Technical Information Center of Denmark

General rights

Copyright and moral rights for the publications made accessible in the public portal are retained by the authors and/or other copyright owners and it is a condition of accessing publications that users recognise and abide by the legal requirements associated with these rights.

- Users may download and print one copy of any publication from the public portal for the purpose of private study or research.
- You may not further distribute the material or use it for any profit-making activity or commercial gain
- You may freely distribute the URL identifying the publication in the public portal

If you believe that this document breaches copyright please contact us providing details, and we will remove access to the work immediately and investigate your claim.

Surface Activity Distribution Measurements and Establishment of a Dose Rate Map inside the Destroyed Chernobyl Reactor

A.V. Chesnokov, V.I. Fedin, A.A. Gulyaev, V.N. Potapov, S.V. Smirnov, S.B. Shcherbak, L.I. Urutskoev, A.G. Volkovich, H. Würz, C.L. Fogh, K.G. Andersson, J. Roed[#]

*RECOM Ltd., Moscow

[†]Interdisciplinary Scientific-Technical Centre SHELTER

[‡]Forschungszentrum Karlsruhe

[#]Risø National Laboratory

Abstract A Gamma Locator designed for contamination survey inside the reactor hall of the 4th unit of Chernobyl NNP has been developed. The device consists of a detector head and a remote control computer connected by a 150 m long cable. The detector head (dimensions: 500mm by 500mm by 400mm; weight: about 40 kg) is a collimated scintillation gamma detector (the collimation angle is 10°). It is installed on a scanning unit and was placed inside the reactor hall. The Gamma Locator scans all surfaces of the reactor hall with angular steps ($\geq 1^\circ$ vertically as well as horizontally) and the particle fluence from the corresponding direction is recorded. The distance between the device head and the measured surface is instantaneously registered by a laser distance gauge. Inside the collimator there is a small CCD camera which makes it possible to obtain a visible image of the measured surface. The effective surface activity levels are presented in colour on the screen of the control computer. The gamma detector essentially consists of a CsI(Tl) scintillator crystal ($\varnothing 8$ mm in diameter, 2.5 mm in thickness) and a Si photodiode. The detector energy resolution is about 8% for radiation from ^{137}Cs . The exposure dose rate distribution in the reactor hall is estimated from the measured effective surface activities (^{137}Cs is the main gamma emitting isotope inside the reactor hall). The results of dose rate calculations are presented in colour superposed on a drawing of the reactor hall.

ISBN 87-550-2444-0
ISBN 87-550-2445-9 (Internet)
ISSN 0106-2840

Information Service Department, Risø, 1999

Contents

Preface 4

1 Introduction 5

2 Description of Gamma Locator 5

2.1 Construction and Main Components of the Gamma Locator 5

2.2 The Main Parameters and Characteristics of the Gamma Locator Systems 7

2.3 Data Presentation Software 10

3 Calibration Procedures 12

3.1 Laboratory Measurements of Apparatus Function of Detectors 12

3.2 The Spectral Characteristics of the Detectors 15

3.3 Test Measurements Inside the Chernobyl Reactor Unit 4 17

4 Measurements Inside the Reactor Hall 22

5 Modelling of Dose Rates 27

5.1 Theoretical Considerations on the Conversion of Measured Spectral Data to Dose Rates. 29

5.2 Calculated Dose Rates inside the Reactor Hall 33

6 Modelling of Forced Dose-Reduction 37

7 Conclusions 39

8 Acknowledgement 40

9 References 40

Preface

This report constitutes the final report for the scientific results of the fixed contribution contract N IC15-CT96-0807 (DG 12-COPE) under the INCO-COPERNICUS program. The project is a continuation of previous work under the INTAS programme.

For the sake of completeness the description of the Gamma Locator developed under the INTAS contract has been included in Chapter 2 of this report.

1 Introduction

The main objective of the project is a measuring of surface activity distribution and establishment of a dose rate map inside the damaged Chernobyl 4 reactor unit. A special device, called the Gamma Locator, has been developed in the frame of the INTAS program to perform these measurements. A detailed description of the Gamma Locator construction and its main systems are presented in Chapter 2 of this report.

The main objective for this period of the project was to finalise the development of the measuring equipment, to calibrate it, to select the location for measurements and to provide an energy supply and communication lines inside the sarcophagus.

Currently, there is a great interest in many laboratories all over the world for development of systems for remote measurement of radioactive contamination levels of equipment and buildings in nuclear enterprises (He *et al.* 1995, Motterhead *et al.* 1996, Sudarkin *et al.* 1996, Simonet 1990 and Chesnokov *et al.* 1994a+b). The majority of the developed systems are based on visualisation of gamma radiation sources (He *et al.* 1995, Sudarkin *et al.* 1996 and Volkovich *et al.* 1990a). These systems are normally based on a position-sensitive detector for high-energy photons. Such systems make it possible to impose a measured intensity of gamma radiation on a visible image of the radiation source on a computer screen and enable only a qualitative estimation of the radiation intensity. Systems comprising collimated detectors (Gamma Locators) are applied to obtain quantitative data on the activity of the gamma radiation source (Motterhead *et al.* 1996, Chesnokov *et al.* 1994, Volkovich *et al.* 1990b and Chesnokov *et al.* 1996). To obtain the gamma image in these systems the position-sensitive detector views the object at different angles in consecutive scans. The spatial resolution is here defined by the angular step of the scanning and by the aperture of a collimator.

2 Description of Gamma Locator

A main feature of the Gamma Locator is the possibility to obtain a radiation energy spectrum. This gives information about the different contaminant isotopes and about the structure of the radiation source. The results of measurements using this type of equipment have been used to generate a computer database of radioactive contamination levels of surveyed objects, which makes it possible to simulate sequences and identify the optimal way to decontaminate the object, to calculate exposure dose rates (EDR) at any point and to predict its change after decontamination. It is also possible to identify doses to decontamination personnel.

2.1 Construction and Main Components of the Gamma Locator

The Gamma Locator was developed recently (Chesnokov *et al.* 1997a) in order to measure surface activities inside the reactor hall of the Chernobyl NPP 4th unit. It consists of two measuring heads and it is controlled by a computer. The main measuring head only differs from that of the version developed under the

framework of the INTAS program (reference number - INTAS-93-2288) by sensitivity. It has the same systems and construction. The second measuring head is similar to the first, but contains no laser distance device (this is the part that is most vulnerable to radiation). The two heads can be operated jointly through the control computer. The second measuring unit is equipped with a small laser, which points to the center of the surveyed surface. The main measuring unit is equipped with a laser distance gauge. This makes it possible to calculate the distance to the measured surface from a knowledge of the relative coordinates of the measuring units and angles to the surveyed object. The construction of the measuring equipment makes it possible to create a model of the surveyed surface, to impose the measured distribution of surface activity on it and to use these data for EDR calculation at any point in space between the surfaces.

The dose potentially absorbed by the measuring head during the complete series of measurements in the damaged reactor hall is high (up to 100 Gray). Therefore, the automated system has the option of using the measuring heads separately in order to reduce the dose they absorb.

The Gamma Locator is an automated, collimated spectrometric detector (CSD) of gamma radiation, which gives information on the energy spectrum of the activity. The main task of this version of the equipment is the measurement of the surface activity distribution with an unknown geometry in the damaged reactor hall of the 4th unit of the Chernobyl NPP, and of any changes to this distribution which may occur during work inside the building.

The CSD includes the following units and systems

- a pan-and-tilt unit that can turn the detector head vertically and horizontally.
- a laser distance device.
- a CCD-camera.
- a spectrum analyser;
- an interface for the CCD-camera
- a control computer.

The measuring head of the Gamma Locator (see Figure 2.1) is designed to enable measurements in areas with dose rates (EDR) as high as 100 mGy h^{-1} . Such high radiation fields impose additional restrictions on devices and their components and significantly reduce the expected lifetime of the electronic equipment. Average surface activities that can be measured by the CSD may be as high as $4 \times 10^{12} \text{ Bq m}^{-2}$ (for ^{137}Cs gamma radiation). This corresponds to a fluence rate in the detector of about $5 \times 10^6 \text{ s}^{-1} \text{ cm}^{-2}$. To reduce the count rate of the detector for higher levels of contamination a 0.125 cm^3 CsI(Tl) scintillator crystal with a photodiode and a collimator with an entrance aperture of 2 mm is used. The count rate of the above mentioned set-up of the detector is some $5 \times 10^3 \text{ s}^{-1}$. To reduce the count rate lead filters are used. Where higher sensitivity is required, in the lower surface activity range between $4 \times 10^6 \text{ Bq m}^{-2}$ and $4 \times 10^9 \text{ Bq m}^{-2}$, a 1 cm^3 CsI(Tl) detector with a collimator with an entrance aperture of $\varnothing 9 \text{ mm}$ is used. The construction of the Gamma Locator makes it easy to rapidly change the lead collimator to reduce or to increase the number of photons incident to the detector.



Figure 2.1 The measuring head of the Gamma locator mounted on a pan-and-tilt unit (to the left). On top of the collimator the laser distance device can be seen.

2.2 The Main Parameters and Characteristics of the Gamma Locator Systems

All systems of the measuring head are mounted on pan-and-tilt tables, which can be rotated in two dimensions (330 degrees horizontally and 180 degrees vertically) and are controlled by PC. The spatial gamma radiation source distribution can be mapped by systematically pointing the detector in different directions. This movement can be programmed and executed automatically by the controlling PC. After the observation, the gamma ray image can be superimposed on the video image obtained by the CCD camera to identify the physical objects associated with the gamma radiation emission. The computer controls all Gamma Locator systems in real time and is also used to process the results.

The Gamma Locator makes it possible to measure ^{137}Cs surface contamination levels between $4 \times 10^6 \text{ Bq/m}^2$ and $4 \times 10^{12} \text{ Bq/m}^2$. This wide range is facilitated through the use of exchangeable detectors of gamma radiation for both measuring heads:

- The detector with scintillator volume of 1 cm^3 is applied at contamination levels between $4 \times 10^6 \text{ Bq/m}^2$ and $4 \times 10^9 \text{ Bq/m}^2$;
- The detector with scintillator volume of 0.125 cm^3 is used at contamination levels between $4 \times 10^9 \text{ Bq/m}^2$ and $4 \times 10^{12} \text{ Bq/m}^2$.
- The spatial entrance angle of the collimated detectors is 10° .

- The measurement time of individual measurements can be varied between 1 s and 10 minutes.
- The distance from the measuring head to the surveyed surface is measured by a laser distance device.

A diagrammatic representation of the Gamma Locator using one measuring head is shown in Figure 2.2. The equipment includes the following basic functional systems:

1. Collimated detector of gamma radiation.
2. Pan-and-tilt unit with control board.
3. Laser distance device.
4. CCD - camera.
5. Unit of communication and management (one on both measuring units).
- 6-7. Computer and software of management to control and record the measured information (one for both measuring heads).

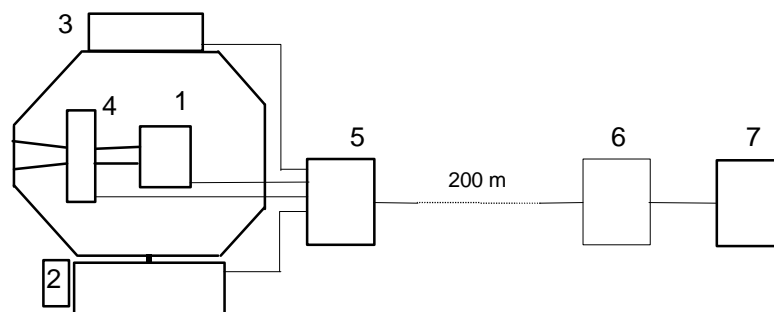


Figure 2.2 Schematic diagram of the Gamma Locator. 1 - collimated detector; 2 - scanning unit; 3 - laser distance device; 4 - CCD camera; 5 - controller; 6 - block of communication and control; 7 - computer.

1. Collimated detector. The detector of gamma radiation is based on the system of a scintillator (CsI (TI)) and a silicon photo diode. It is placed inside a lead shielding (the thickness of the lead shielding is about 60 mm) with a collimator, to shield against extraneous radiation. The detector is supplied with a preamplifier, a shape amplifier and input and output connectors. It is constructed as a separate unit. The preamplifier of the detector and the shape amplifier are made as separate units and are located inside the lead shielding of the detector to reduce radiation doses to electronic systems and chips as much as possible.

2. Pan-and-tilt unit with control board. The pan-and-tilt unit (VPT-50/24-POT) is a remote controlled unit for adjusting the orientation of the detector head in both horizontal and vertical direction. It is a weatherproofed version manufactured by Videor Technical of Germany. There are two electrical motors (horizontally and vertically rotating) and two discrete gauges of angular movement (horizontal and vertical rotation). The scanning angles are 0 to 360° horizontally and -90° to 90° vertically. The error on a single angular movement does not exceed 0.3° at a rotation speed of 6.25 degrees per second in the horizontal plane and 2.5 degrees per second vertically. The pan-and-tilt unit can carry a load of 35 kg and it does not require additional counterweights or springs. Its centre of gravity is displaced. The total weight of the unit is 9.5 kg. It is reliably protected

from various types of natural influences, such as a wind, snow or ice. The pan-and-tilt unit can be used from -20 to 80 °C.

3. Laser distance device. The laser distance device is applied to measure distances from the Gamma Locator to the surveyed object. The principle of its function is based on a time measurement of a light beam passage from the laser up to the object and back. The range of distances that can be measured generally goes from 10 m to 100 m. The maximum errors of measurement are :

- systematic error - $0.1 \text{ m} + 0.2 \% D$ (where D is the measured distance, m);
- uncertainty - 0.2 m.

At distances of less than 10 m the error becomes significant.

The laser is used to identify the centre of the area of the gamma measurement. It is only established on one of the CSDs. The light spot of the laser (laser pointer) can be observed by the CCD-camera inside the measuring head. The main features of the applied laser are the small size and the relatively great power. The laser has the dimensions of $\varnothing 20 \text{ mm}$ and 60 mm in length. The power of the laser beam is 2.5-3 mW. The laser beam can be followed visually at distances up to 50 m. The small laser size makes it possible to shield the device with lead, if necessary.

4. CCD-camera. In order to view the physical shape of the surveyed objects a black-and-white CCD-camera MTV-261EM/CM (one on each measuring head) is used. This CCD-camera is chosen because of its small size (50×50×30 mm), which makes it possible to shield with lead, to protect against the radiation. With this design the camera can be operated for relatively long periods of time, with high levels of radiation, as is the case inside the damaged reactor hall. The CCD-camera has automatic adjustment of brightness and an objective with short focus, that provides a precise video image of studied objects.

5. Controller. The controller is used for processing signals and for control of the pan-and-tilt unit. The controller is based on a receiver (PTZFI/C-EN) and produced in a weatherproofed version. This unit makes it possible to remote control the pan-and-tilt unit with fixed or variable rotation speed. The communication between the PTZFI/C-EN and a transmitter (PTZFI/C-S8) is made through two coaxial cables of 200 m length. In addition, if necessary, the controller makes it possible to operate with a video camera.

6. Block of communication and management. The communication block transfers all information about the current condition of the scanning unit (horizontal and vertical angles of rotation, application, etc.), the signal of the detector and the video image to the computer.

Shapers of received signals from the controlling computer, amplification of signals to the computer (up to an adequate level for transfer through 200 metres long cables), the power supply and the printboard for the spectral analyser are also located inside this block.

6a. Transmitter PTZFI/C-S8. To switch the CCD-camera and transmit a television signal, a transmitter (PTZFI/C-S8) is used. The PTZFI/C-S8 is a consecutive eight-channel video switch. The transmitter has a wide set of additional functions (such as the program switch on and off, an alarm-switching, etc.). The presence of 8 video channels makes it possible, if desired, to easily increase the number of controllable collimated detectors from two to eight. The PTZFI/C-S8

has an RS-232 interface, which provides direct communication with the controlling computer.

7. Controlling computer. This PC is used to control all the systems mentioned above. To import the video image into the computer a board for digitalisation of the video signal is used. This is installed inside the controlling computer. The specially developed software makes it possible to control all systems, to switch on and off separate parts, to record data on a disk, to show it on the screen and to process the measured data completely. The measured distances are also shown on the computer screen. The measured surface activity, presented with a colour palette, can be super-imposed on the video image of the investigated objects obtained by the CCD camera, and the total picture is displayed on the computer screen. The software makes it possible to process the video images.

To co-ordinate separate parts of the equipment, video ground-loop correctors (VT1117) are used.

Using the equipment specified above it is possible to supervise conditions in the location of the collimated detector, on the video monitor and on the screen of the controlling computer.

2.3 Data Presentation Software

In the frame of the INCO-COPERNICUS project a computer program (3DVIEWER) was developed, which can be used to visualise all data obtained in the reactor hall of the Chernobyl NPP 4th unit. This program, which was run on an IBM PC with WINDOWS 95, uses the Borland run time library BC450RTL.DLL and the following two data bases:

MDB.CZ - measured data, including effective ^{137}Cs surface activity density (deposition) and coordinates of the investigated surface;

EDR.CZ - calculated effective dose rate (EDR) in the surveyed reactor hall.

A series of photos (BMP-files) of the reactor hall may be used by 3DVIEWER to show data superposed on visible images.

The program has 4 windows for data presentation and guidance on the computer screen:

- the main window;
- the draw window;
- the information window;
- the status bar window.

The main window is always displayed. The user may show or hide all other windows by pressing 'hot keys' on the keyboard: key F3 for draw window; key F4 for information window; key F2 for status bar window.

The main window is used to show the three-dimensional view from any view point in any direction with a view angle within the range of 10 - 80 degrees. The shown data include:

- a model scheme of the reactor hall;
- distances for the model scheme;
- distances for the measured surfaces;
- measured ^{137}Cs deposition;
- calculated EDR in the surveyed region;
- photos of the central hall.

The selection of the data to be shown is made from the program menu.

All data are presented and described in Cartesian coordinates (absolute system). The X-axis of the absolute system is directed from South to North, and the Y-axis from East to West. The Z-axis is in vertical direction.

For the model scheme of the reactor hall the following dimensions were used: The South and North walls of the reactor hall correspond to $x=12$ and 36 m, approximately. The East wall of the reactor hall lies in the plane $y=0$, whereas the West wall has the co-ordinate $y=54$ m. It has been established that before the accident, the floor in the reactor hall lay at the level $z=0$ and the roof of the constructed sarcophagus is at the level of $z=27$ m. The vertical axis of the destroyed reactor has the horizontal co-ordinates of $x=24$ m, $y=42$ m.

The image is displayed in this 'view' co-ordinate system. The viewpoint is the origin of this system. In order to pass from absolute system of co-ordinates to the view system, the origin of the co-ordinate system must be transferred to the view point, then the co-ordinate system must be rotated counter-clockwise around the z-axis by the angle Fz , around the y-axis by the angle Fy , and around the x-axis by the angle Fx . Thus, Fz and Fy angles are the horizontal and vertical angles of the spherical co-ordinate system. The angle Fx corresponds to image rotation in the view direction. The user may change the view parameters by pressing 'hot keys', or by using the view dialogue panel from the program menu.

The EDR image is formed for a x-, or y-, or z-cross section in a rectangular window. The EDR cross section window size and position are established by the user from the dialogue panel for EDR options under the program menu.

The iso-line values, which are displayed for the contamination level, distance or EDR data, are selected from the program menu.

The draw window, information window and status bar window are used to describe the image in the main window.

The draw window can be used to obtain horizontal and vertical cross section drawings of reactor hall. This window shows the viewpoint position in the reactor hall, the direction of view, size and orientation of the image in the EDR window. The Gamma Locator position in the reactor hall is also shown in the draw window.

The information window describes the shown system and its parameters (colours and iso-line values).

The status bar window contains information about the current view point position, direction and angles of view.

Fig. 2.3 shows an example of a computer screen during operation.

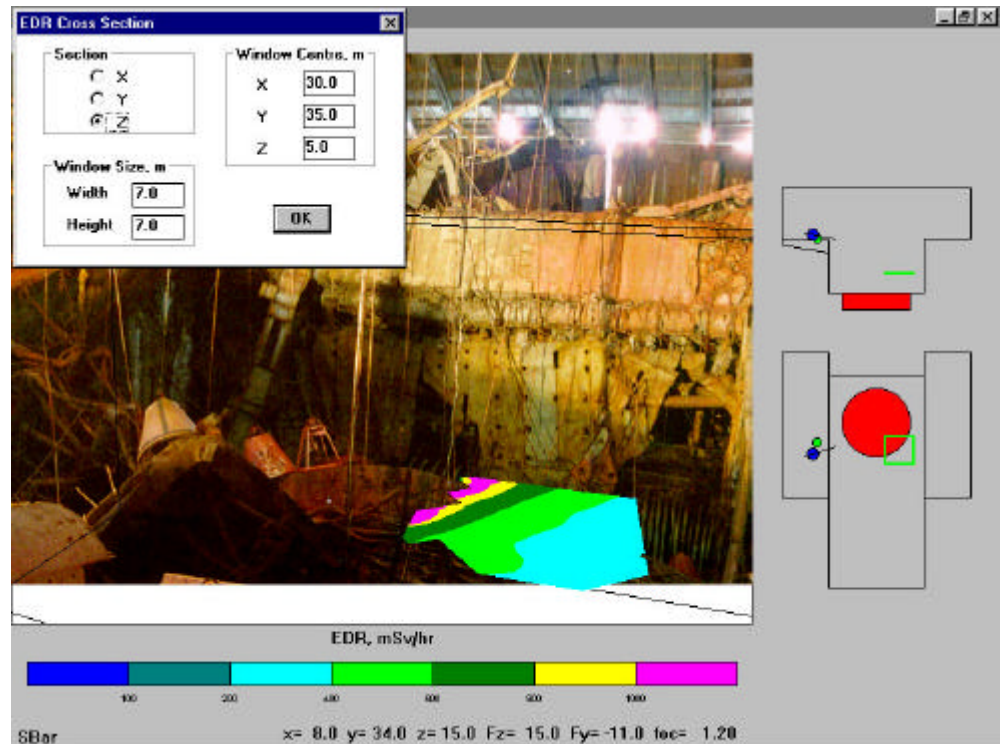


Figure 2.3 Example of how the EDR results may be presented superposed on photographic pictures.

3 Calibration Procedures

3.1 Laboratory Measurements of Apparatus Function of Detectors

To determine the sensitivity and angular apparatus functions of the Gamma Locator detectors, test measurements were carried out in the laboratory using plane and point sources of ^{137}Cs (gamma photon energy : 662 keV).

The activity of the ^{137}Cs point source was about $3 \cdot 10^9$ Bq. The source was placed at a distance of about 5 m for the test of the more sensitive detector (scintillator volume: 1 cm^3) and at a distance of about 1 m for the less sensitive detector (scintillator volume: 0.1 cm^3). These distances provide a sufficiently high count rate for the detectors to eliminate the influence of geometrical factors. The Gamma Locator was scanning an angular segment of 40° by 40° , where the source was placed at the centre. The angular step size of the scanning was 1° .

The angular apparatus functions of the detector were defined from these measurements. The image of the radiation source seen from the detector with the CCD camera is shown in Figure 3.1, with the measured distribution of radiation superimposed.

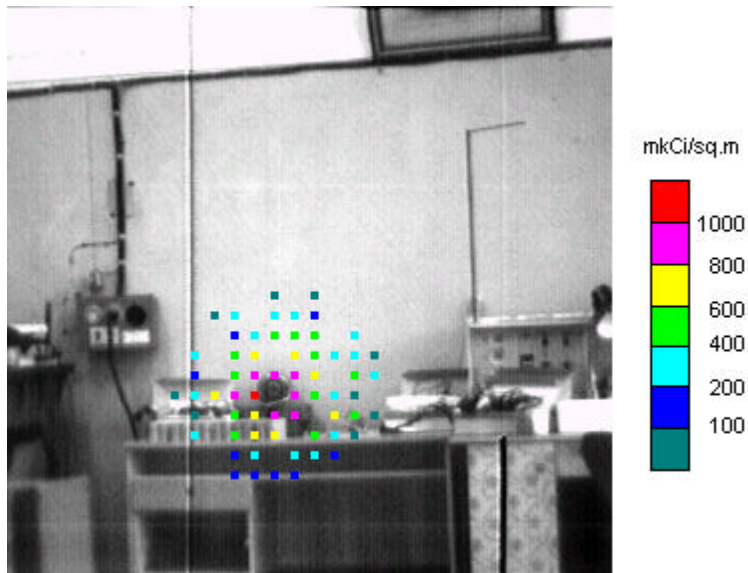


Figure 3.1 Visible images and gamma measurements of the point source (angular size : ca. 0.1°). An angular step size of 1° was used for the scanning.

The apparatus function of the large volume detector is shown in Figure 3.2. Here, it is seen that the angular width of the measured peak at half height of maximum (FWHM) is 6° . Similar data were obtained for the smaller detector, for which the angular FWHM was found to be 7.5° (see Figure 3.3). The function shown in Figure 3.2 is not as smooth as could perhaps be expected. This is not a result of any statistical error of the measurements as such. Rather, the unevenness of the function illustrates the great sensitivity of the detector response towards small deviations in the operation of the pan-and-tilt unit. The accuracy of the pan-and-tilt unit adjustment is better than 0.3° on a single step, but an error can gradually accumulate and may be as high as 1° - 2° on large angular segments when scanning at 1° steps. Thus, the error in connection with the installation of an angle substantially exceeds the statistical error of the measurement (the integral count number in the main part of the spectrum exceeds 2000, corresponding to a standard deviation of less than 2.2 %).

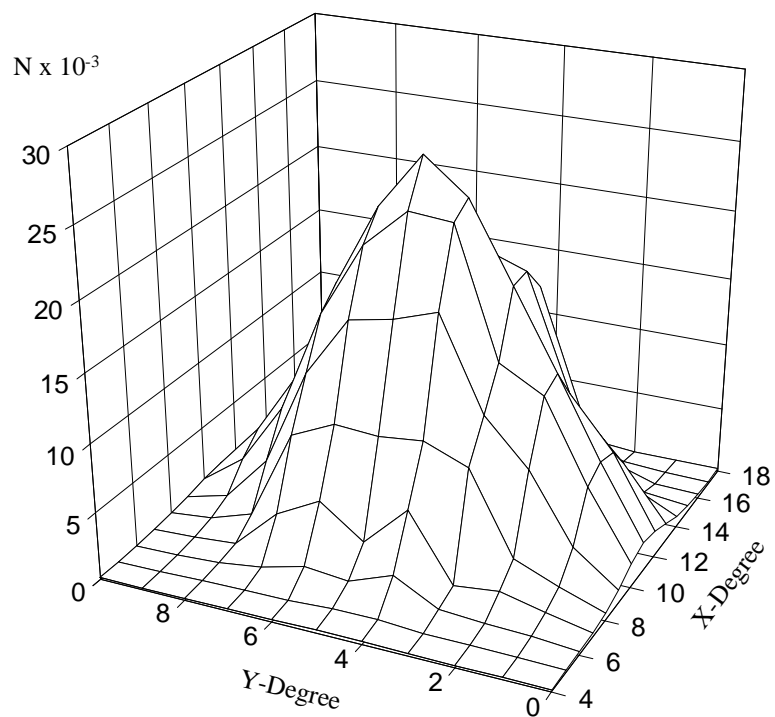


Figure 3.2 Angular apparatus function of the large volume detector. The number of counts is shown as a function of angular steps in two dimensions.

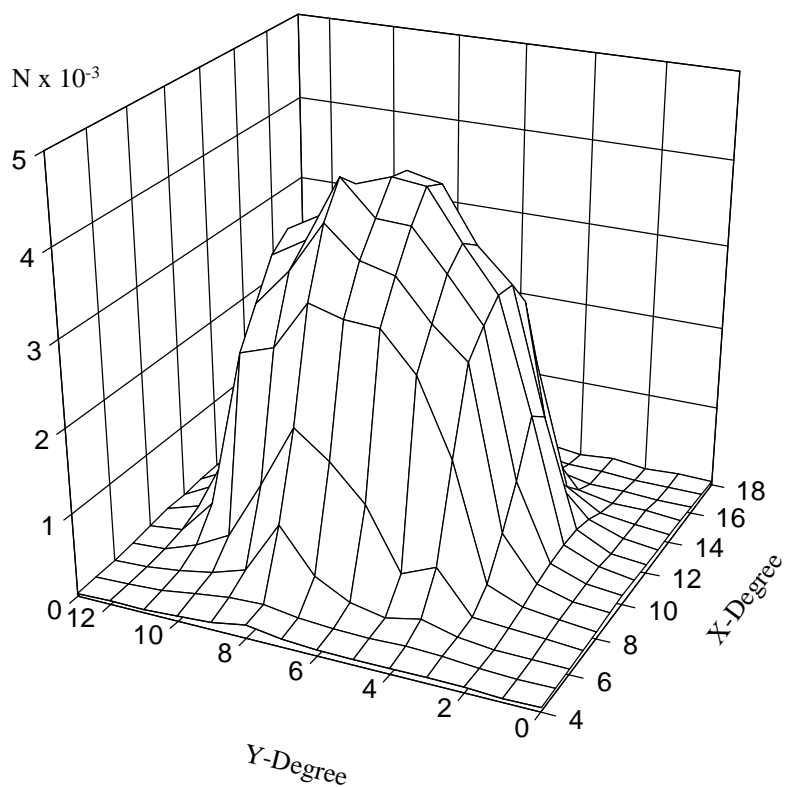


Figure 3.3 Angular apparatus function of the small volume detector. The number of counts is shown as a function of angular steps in two dimensions

The resolution of both detectors at one tenth of maximum (FWTM) was found to be 10° . The resolution of the large detector at 80 % of the maximum was found to be 2° , whereas it was found to be 4° for the smaller detector. The better resolution of the large detector makes it well suited for accurate determination of the position of for instance point sources.

The calibration of the detectors was carried out using a plane homogeneously distributed source of ^{137}Cs measuring 35 cm by 35 cm. The distance between the source and the detector was 0.25 m. At this distance, the plane source was, due to the detector collimation, sufficiently large to simulate an infinite area. The manufacturing and certification of the source was carried out at a special Russian certification enterprise in 1992. The surface activity of the created plane source was 555 MBq/m^2 at the time of the certification. The heterogeneity of the activity distribution over the plane source was found not to exceed 6 %.

3.2 The Spectral Characteristics of the Detectors

The calibration spectrum for the plane calibration source, as measured with the small detector, is shown in Figure 3.4. The distance between the source and the entrance window of the measuring unit was 0.25 m. The exposure time was 10800 s. The energy resolution of the detector was found to be about 8% (for the 662 keV energy peak of ^{137}Cs radiation) and this is sufficient to obtain information about the sources of gamma radiation inside the damaged reactor hall. Also the background spectrum (i.e. the spectrum obtained without any sources present) was measured and used to correct for the contribution of naturally occurring radionuclides and cosmic radiation in the calibration spectrum. The calibration data was used in the calculation of surface activity and exposure dose rate (EDR) distribution.

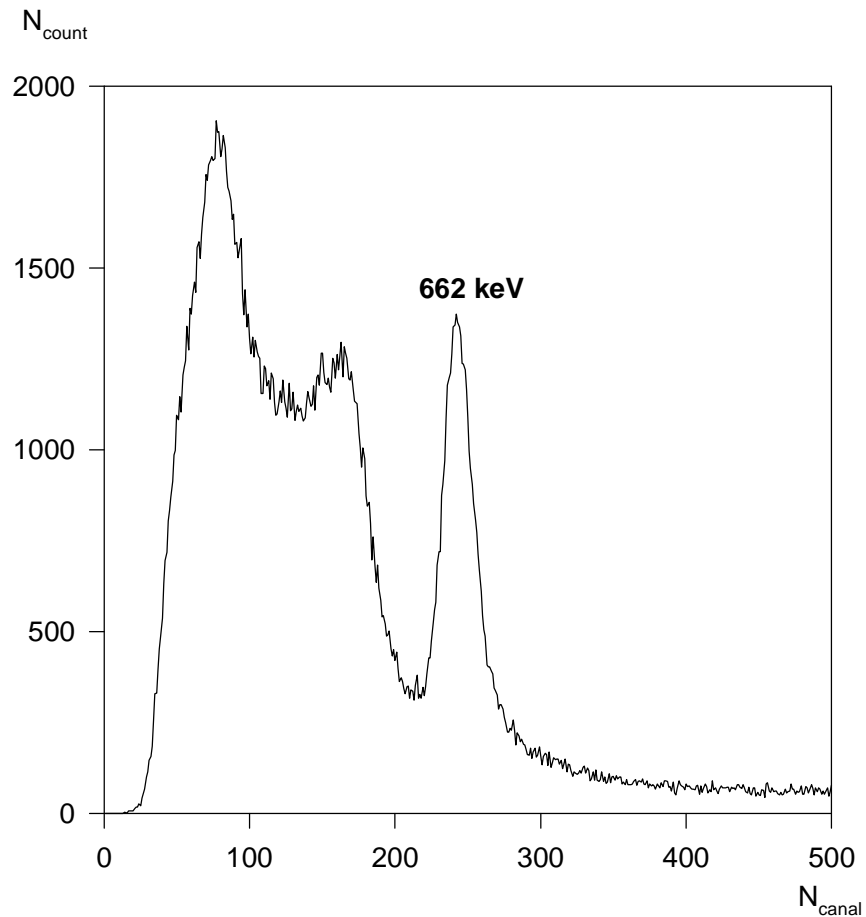


Figure 3.4 The calibration spectrum of the small detector.

To verify the calculation of the EDR level in the laboratory, three point ^{137}Cs sources of different activities were placed in the room. The entire room (4π solid angle) was scanned with the Gamma Locator. The distances to surfaces and the corresponding distribution of the surface activity in the room were measured. This data was used as input for a special computer programme, which calculated the EDR distribution at a height of one meter above the floor of the room. The obtained result is shown in Figure 3.5. The difference between the calculated distribution and measurement data obtained with a standard dosimeter at separate points was found to be less than 20 %. The greatest deviations were observed for small distances from the point sources ($r \leq 0.5$ m).

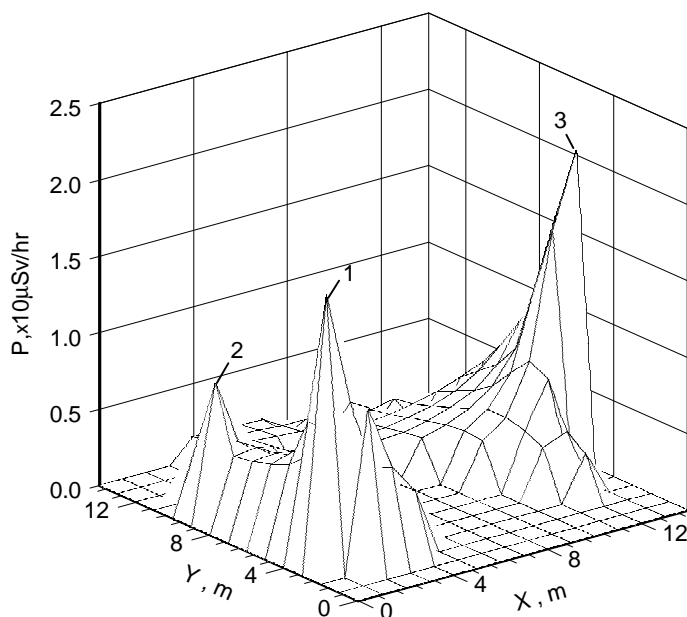


Figure 3.5 EDR (in units of 10^3 's of $\mu\text{Sv h}^{-1}$) distribution calculated for a height of one meter above the floor in the laboratory room. Three peaks are indicated.

3.3 Test Measurements Inside the Chernobyl Reactor Unit 4

The control system for the Gamma Locator was installed in room N 554 of the 4th unit of the Chernobyl NPP. The exposure rate in this room was about 2 mR h^{-1} . This room was used as a control centre for the measurements in the reactor hall.

A sample containing nuclear fuel debris was obtained to study the characteristics of the measured spectra. This sample was taken from the reactor hall for testing in the laboratory. It was placed in a special lead container. The Gamma Locator was placed at the distance of 5 m from the sample. The gamma spectrum of the sample was measured with the Gamma Locator and stored. A video image of the sample, as recorded with the video camera of the Gamma Locator, is shown in **Error! Unknown switch argument.**. The white circle shows the position of the gamma emitting sample identified with the Gamma Locator.



Figure 3.6 The CCD camera picture of the measurements in the room N 554 with the position of the sample shown as a white circle.

The gamma spectrum obtained for this sample with the Gamma Locator is shown in Figure 3.7. It can be seen that the main gamma emitting isotope is ^{137}Cs . The rather large low-energetic part of the spectrum is caused by scattering of gamma radiation inside the nuclear debris sample and in the Gamma Locator. The increased scattering in the volume sources inside the reactor hall was taken into account in the calculations of the EDR distribution inside the reactor hall.

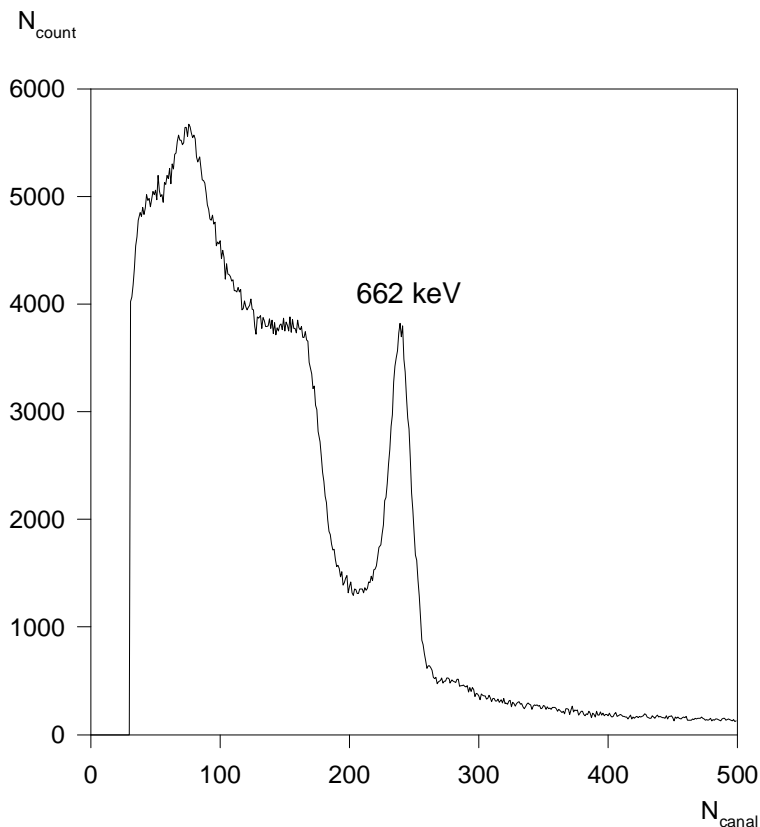


Figure 3.7 The radiation spectrum obtained by the Gamma Locator in room N 554. The number of counts is shown as a function of the energy-dependent channel numbers.

The definition of the surface activity of ^{137}Cs , σ , based on the total count rate, is not quite correct due to the large contribution of high-efficiency detected low energy photons to the count rate of the detector.

As the measurements were carried out by the energy spectrum recording detector other approaches for definition of the surface activity are possible.

The first approach is based on a determination of the counts in the full energy absorption peak N_f ($\Delta = 600 - 740$ keV). It is obvious, that

$$\sigma = \text{const } N_f$$

where the value of the constant is found from the calibration of the detector on a smooth surface source with known activity.

However this approach has a shortcoming in relation to measurements in the reactor hall, due to the presence of volume sources, rather than surface sources of radiation. With a volume source a significant part of the unscattered (direct) radiation is absorbed. Therefore the estimation of σ will in this case underestimate the surface activity.

It is known, that more than 95 % of the EDR is due to the radiation from contaminants located in a surface layer of a thickness of 3 mean free paths (mfp) of photons with energy 662 keV. Therefore, in the case of volume sources, the surface activity is the total ^{137}Cs activity per unit of the surface area coming from a layer with a thickness of 3 mfp. This is the main dose contributing activity.

To define the activity from a 3 mfp thick layer, it is necessary to use other energy ranges of the recorded energy spectrum. In Fig. 3.8 the recorded spectra are shown of the detector with the scintillation crystal thickness of 2.5 mm, detecting the radiation on a surface (curve 1) and homogeneously distributed in con-

crete (curves 2-4) of thicknesses of 1, 2 and 3 mfp, with identical total activities per areal unit.

N, r.u.

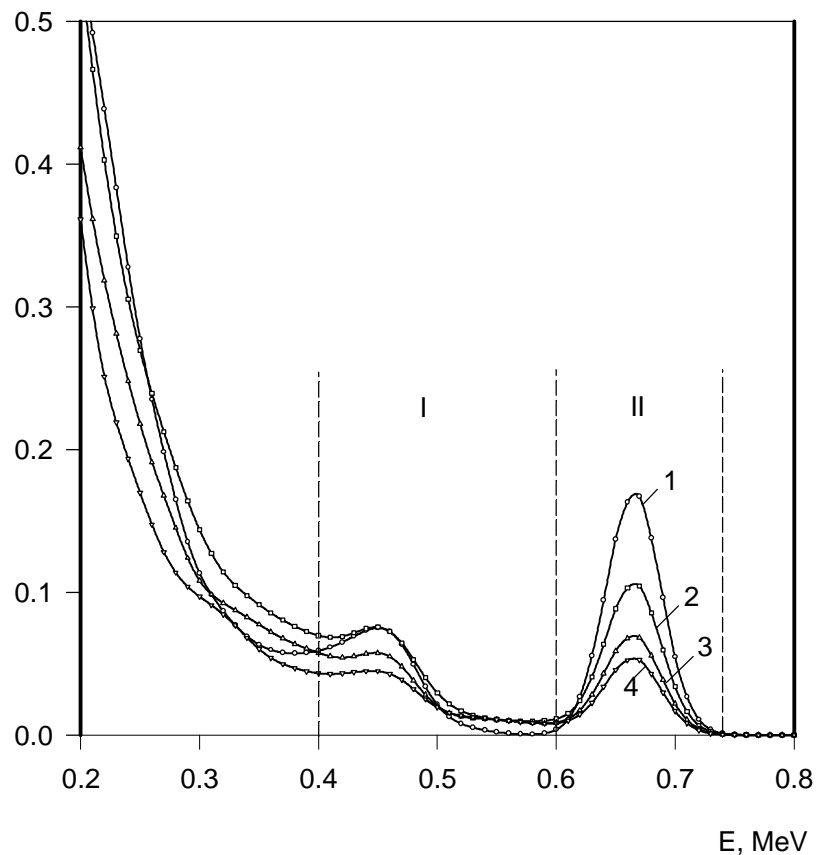


Figure 3.8 An energy spectrum recorded with the detector, detecting the radiation from a surface source (curve 1) and of homogeneously distributed activity in concrete layers of 1 mfp (curve 2); 2 mfps (curve 3) and 3 mfps (curve 4). The number of counts is shown as a function of the energy in MeV.

As can be seen from Fig.3.8, in energy range II (the peak of full energy absorption) the count rate decreases markedly with increasing thickness of the layer throughout which the source is distributed, whereas energy range I is characterised by a relatively invariable count rate. The dependence of the count rate in energy range I on the thickness of the source layer is shown in Fig. 3.9, relative to the count rate from a surface source. As can be seen from this figure, the change in the count rate with increasing source thickness does not exceed 25 %.

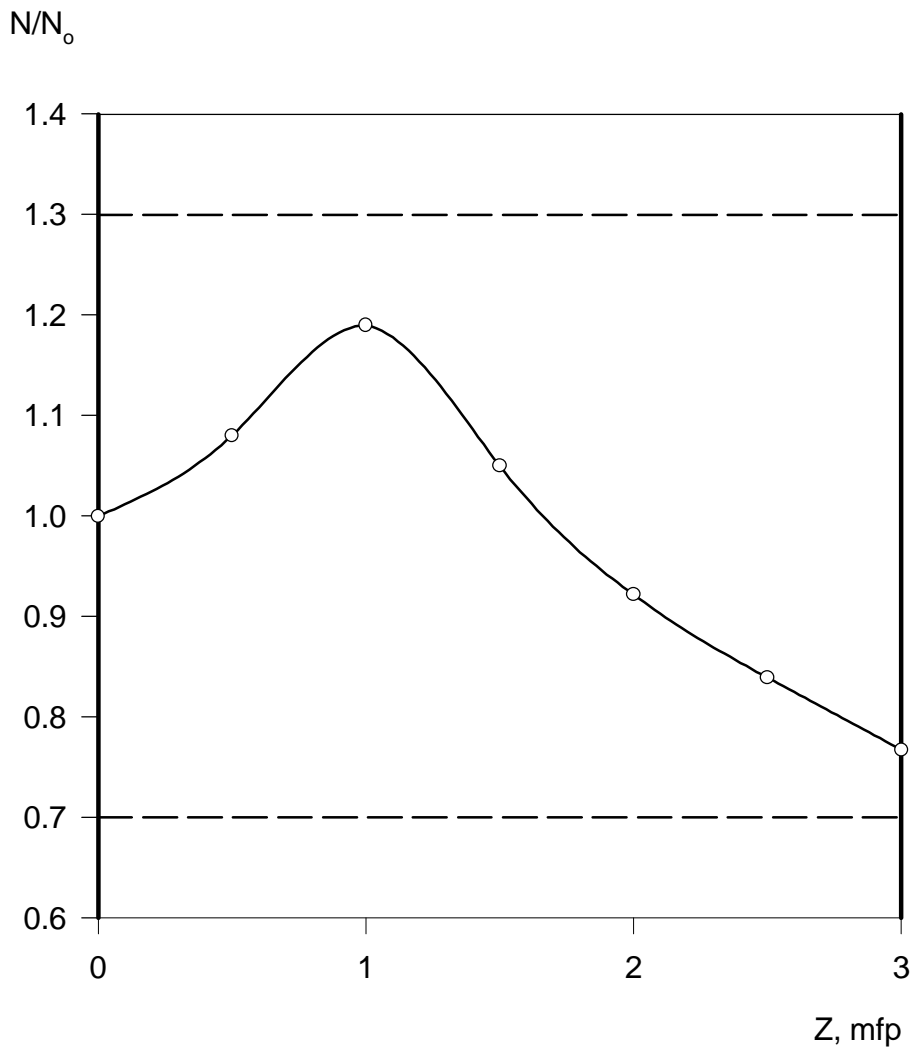


Figure 3.9 Dependence of the relative count rate in spectrum range I on the thickness of the source layer Z (expressed in mfp units). N_0 is the corresponding count rate from a smooth surface source.

Thus, to define the main dose contributing ^{137}Cs activity per unit of surface area, it is possible also to apply an expression of the type:

$$\sigma = \text{const } N$$

where N_c is the number of counts in the 400-600 keV window (energy range I), and the value of the constant could also be established from the calibration of the detector with a surface source of known activity.

4 Measurements Inside the Reactor Hall

The Gamma Locator was installed inside the reactor hall of the 4th unit of the Chernobyl power plant. Figure 4.1 shows a picture taken during the installation of the device in the reactor hall. The light visible in the upper centre of the picture is due to the leaks in the sarcophagus. The umbrella seen in the picture was positioned to protect the gamma locator from the falling moisture in the reactor hall. The moisture is partly due to leaks in the roof and partly from the spraying of water in the reactor hall to reduce resuspension of dust. Figure 4.2 shows an example of the sort of images that can be obtained of physical objects with superposed surface activity colour patterns. The position of the Gamma Locator in the reactor hall is mapped in Figure 4.3. From this position it is possible to scan most of the reactor hall. Especially, there is a good view of the top of the reactor core and the reactor cover. The dose rate in the reactor hall is highest around these objects and it is thus expected that the most intense sources will be in this area. The reactor cover stands in a nearly vertical position after the explosion. The cover has a diameter of 18 metres and it is 3 metres thick. From this location all surfaces of the building were scanned with an angular step of 5°. The activity distribution in the reactor hall is very heterogeneous and in some directions, a significant fraction of the photons, which are registered by the detector, passes through the collimator shielding of the CSD. Therefore, it was necessary to measure this background separately. Measurements in which the collimator was closed by a lead shutter were carried out with the same angular step to determine the influence of these photons. The energy spectrum was recorded in the computer at each position of the pan-and-tilt unit. The background spectrum (with shutter) was subtracted from the main spectrum (without shutter) to determine the surface activity at each position of the collimated detector. Thereby, the surface activity distribution was recorded. Figure 4.4 shows the main (1) and background (2) spectra obtained by measurement at the most heavily contaminated place in the reactor hall.

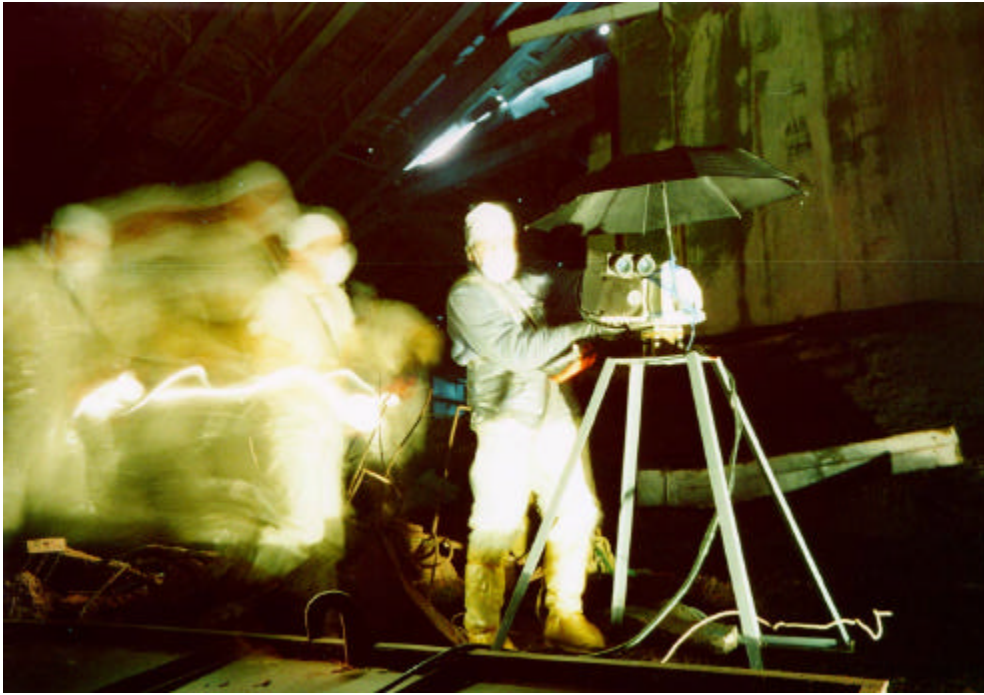


Figure 4.1 The measuring head of the Gamma Locator under installation in the reactor hall.

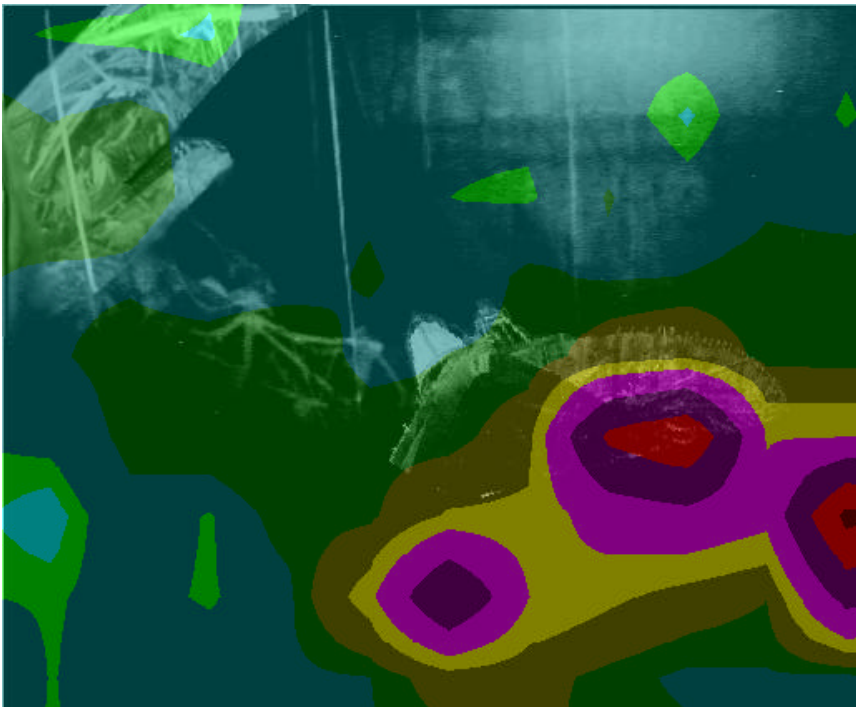


Figure 4.2 The superposition of colour level of surface activity on a visible image of the destroyed reactor.

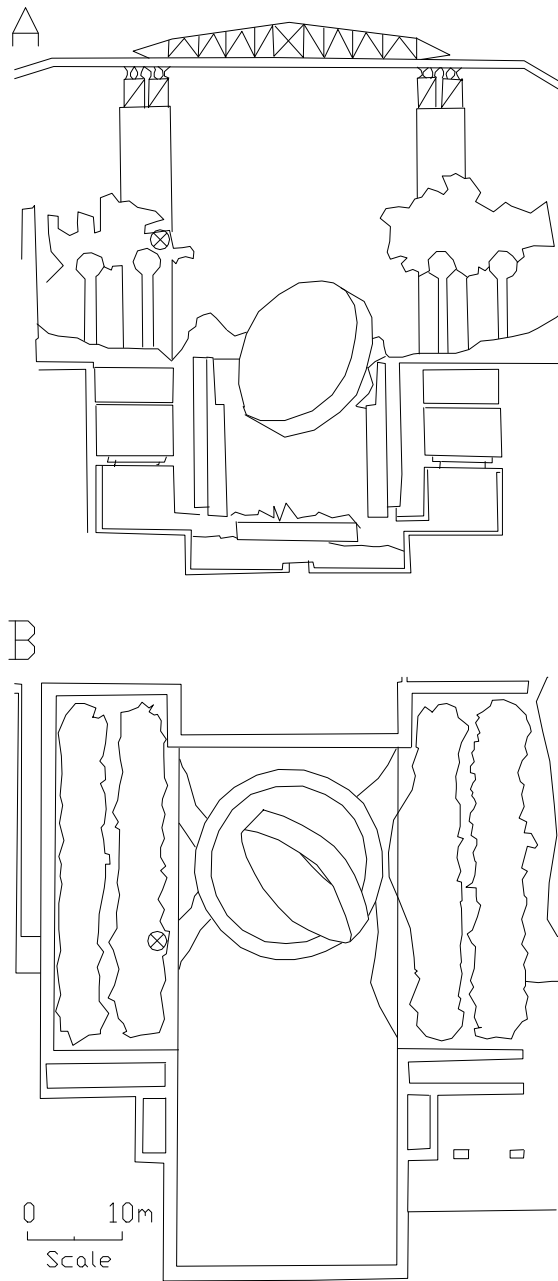


Figure 4.3 A: Cross section along the axis of the destroyed reactor; B:- Horizontal cross section at a level of 43 m above ground.

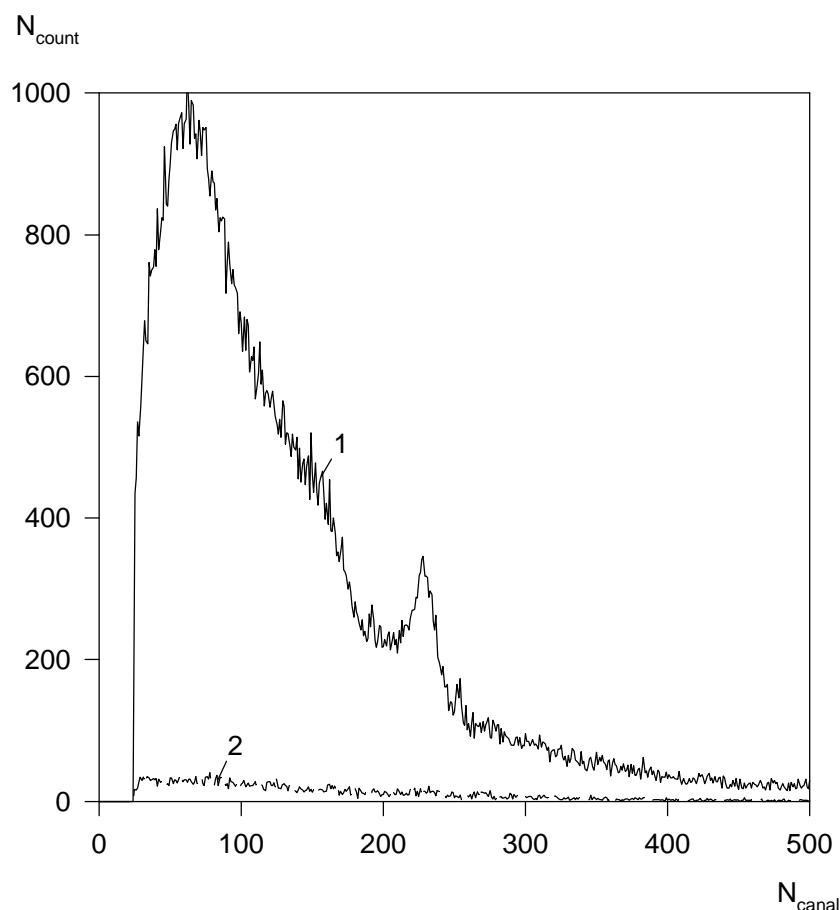


Figure 4.4. Gamma energy spectra measured at the most heavily contaminated area in the Chernobyl reactor building.

In addition to the scanning with 5° steps, the surfaces with the highest contamination were scanned with an angular step of 1° . Using the device calibration described above, the surface activity distribution was calculated for each spectrum. The obtained maps of the surface activity distribution were superposed on the images obtained with the CCD camera. In this way it was possible to identify the objects that were the most intense sources of radiation. In the picture in Figure 4.2 the camera is pointed towards the area around the open reactor, and a surface activity map is superposed on it. Not surprisingly, the main contributing source to the dose rate inside the destroyed reactor is in this area.

The distribution of the contamination is shown in Figure 4.5, in the angular coordinates ϑ from -85° to $+90^\circ$ and φ from $+31^\circ$ to $+356^\circ$. An estimate of the angular activity distribution based on the whole energy spectrum from 50 to 1500 keV is shown in Figure 4.5 A, whereas Figure 4.5 B shows an estimate based on the full energy peak (600-740 keV). Figure 4.5 C shows an estimate based on the counts registered in the energy range from 400 to 600 keV, corresponding to a Compton scattering part of the spectrum. The main part of the activity is located in the area of the destroyed reactor ('scheme Elena'). An analysis of the spectrometric data has shown, that the contaminated area must be regarded as a volume source, and due to self-absorption, the estimate of the activity which was based entirely on the full energy peak underestimates the result by a factor of 2.5 - 3 compared with the estimate which is based on the Compton scattered part of the energy spectrum (400-600 keV). The estimate based on the total spectrum overestimates the activity due to the influence of the scattered and reflected radiation. The average surface activity near 'scheme Elena' was found to be as high as $4 \cdot 10^{12}$ Bq/m². The places with the highest sur-

face activity were scanned with an angular step of 1° . In this case, one energy spectrum was recorded for each segment of 3° by 3° . The surface activity distribution was superposed onto a colour image of the destroyed reactor ('scheme Elena'). The total activities of the three strongest sources are $\sim 6 \cdot 10^{13}$, $\sim 12.5 \cdot 10^{13}$ and $\sim 18 \cdot 10^{13}$ Bq respectively.

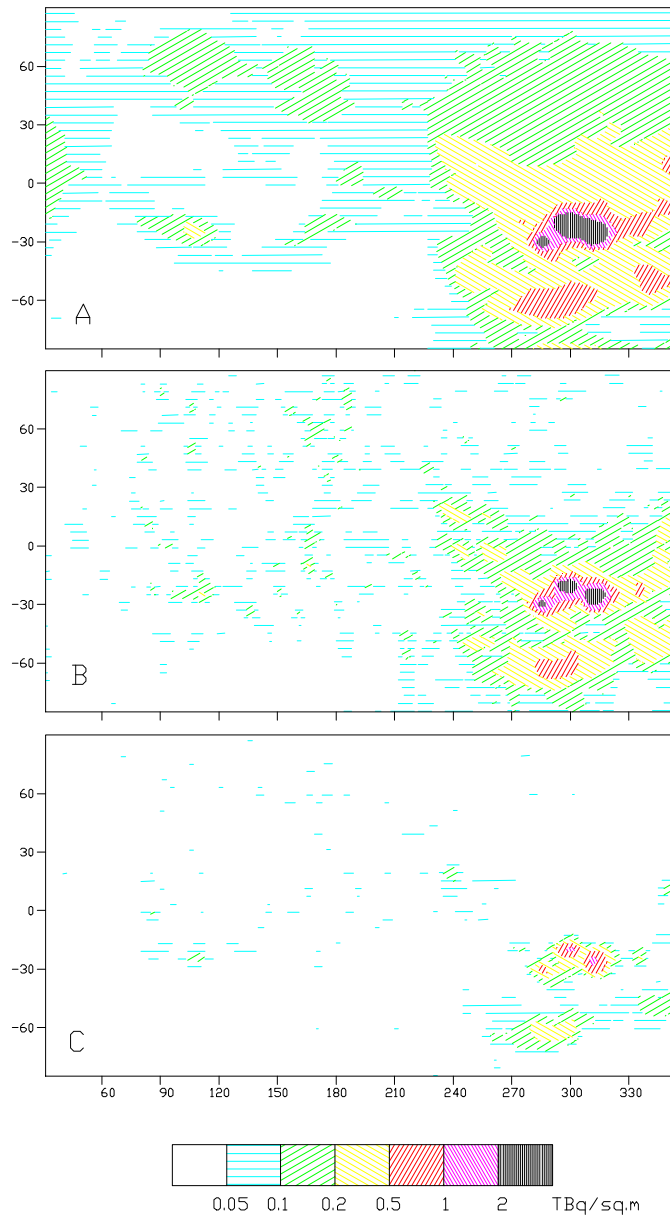


Figure 4.5 Angular surface activity distribution in the reactor hall.

5 Modelling of Dose Rates

The method for calculation of the EDR distribution inside contaminated buildings is described by Chesnokov *et al.* 1997b. This method works well, when the contamination is located on surfaces. However, as previously mentioned, the measurements carried out by CSD in the reactor hall have shown that several sources have the character of volume sources, which demand changes in the above-mentioned method.

For each measuring position of the Gamma Locator the radiation spectrum with and without shutter was recorded by the computer. To determine the surface activity, first of all, the background spectrum (with shutter) was subtracted from total spectrum (without shutter) and using the 3 energy ranges mentioned above, the surface activity was calculated.

The next problem is connected with the presence of volume radiation sources, either in the form of larger pieces of the reactor core scattered by the first explosion during the accident, or by subsequent covering of sources by absorbing materials. Photons are scattered and reflected inside the covering materials, depositing their energy, as illustrated in Figure 5.1. Due to this repeated scattering and reflection the photon energy decreases. This increases the efficiency of its detection by the crystal.

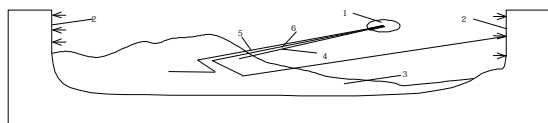


Figure 5.1 Geometry of Gamma Locator measurement in a complex structure of radiation sources. 1 - Gamma Locator; 2 - surface radiation sources; 3 - volume radiation source; 4 - flux of non-scattered radiation; 5 - flux of repeatedly scattered radiation; 6 - flux of reflected radiation.

For Gamma Locator measurements in the intensive radiation fields, the scintillation volume is decreased to reduce the count rate of the detector. This was the case for the measurements inside the reactor hall, where the thickness of the scintillation crystal in the direction of the axis of the collimator was 2.5 mm. In Table 5.1 the measured detection efficiencies of detectors with specified sizes are given for photons of 60 and 600 keV energy. It can be seen from Table 5.1 that for the smaller detector the efficiency of low energy radiation detection is much higher than that for high-energy radiation. This greatly influences the detected spectrum of radiation.

Table 5.1 Efficiencies of two detectors of different sizes, at different photon energies.

Energy keV	Efficiency of detection	
	thickness of 2.5 mm	Thickness of 10 mm
60	0.998	1.00
600	0.087	0.301

In Figure 5.2 an energy spectrum obtained with the Gamma Locator with the geometry shown in Figure 5.3 is presented. From this figure it can be seen that for the detector with a crystal thickness of 2.5 mm the contribution of scattered radiation is 90 %. Therefore the estimation of surface activity and EDR calculation based on an integrated count rate will be incorrect. In this case it is necessary to take into account the radiation spectra to calculate the EDR distribution.

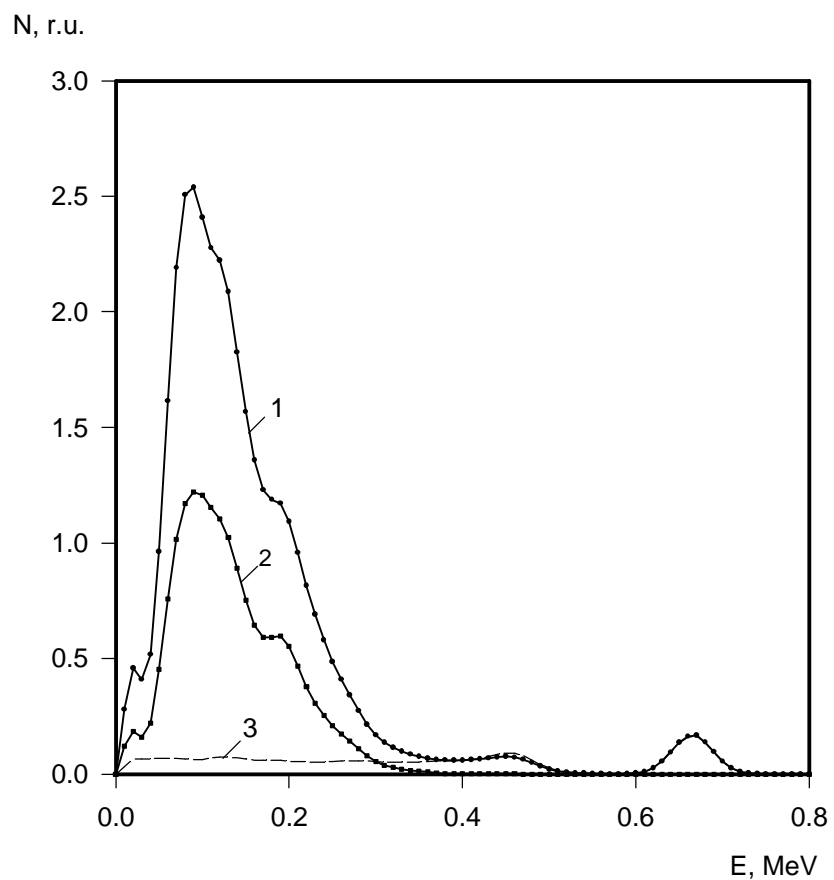


Figure 5.2 Energy spectrum obtained with the Gamma Locator, calculated for geometry of measurements. 1 - is the total spectrum, 2 - is the contribution from reflected radiation (45 %) and 3 - is the contribution of non-scattered (direct) radiation (10 %).

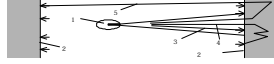


Figure 5.3 Schematic representation of the location of Gamma Locator (1) and plane sources of radiation (2) for numerical simulation of an apparatus spectrum. Components of detected radiation: 3 - non-scattered (direct) photons; 4 - repeatedly scattered photons; 5 - reflected photons.

5.1 Theoretical Considerations on the Conversion of Measured Spectral Data to Dose Rates.

The main factor which characterises the radiation field is the angular and energy differential flux of photons $\Phi(\vec{r}_0, \vec{\Omega}, E')$, as defined by Mashkovich, 1982. Assume that the Gamma Locator is located at the point \vec{r}_0 . The spectrum, $N(E)$, recorded by the detector located in the radiation field may be described by the formula:

$$N(E) = \int_{\Delta\Omega} d\vec{\Omega} \mathbf{j}(\vec{\Omega} \vec{\Omega}_0) \int_0^{E_0} dE' G(E, E') \epsilon(E') \Phi(\vec{r}_0, \vec{\Omega}, E'), \quad (1)$$

where $\mathbf{j}(\vec{\Omega} \vec{\Omega}_0)$ is the angular apparatus function (see Figure 5.2), $\vec{\Omega}_0$ is the direction of the detector's collimator axis, $\epsilon(E')$ is the total detection efficiency of photons as a function of their energy, $G(E, E')$ is the detector response function for detection of photons of the energy E' , E_0 is the maximum photon energy and $\Delta\Omega$ is the solid angle of the collimator.

The photon flux in the solid collimator angle $\Delta\Omega$ at the point \vec{r}_0 determines the exposure dose rate (EDR) $\Delta(\vec{r}_0)$, which is expressed by the formula:

$$\Delta(\vec{r}_0) = \int_{4\pi} d\vec{\Omega} \int_0^{E_0} dE f_a(E') \Phi(\vec{r}_0, \vec{\Omega}, E') \quad (2)$$

Here $f_a(E)$ determines the EDR as a function of photon energy, expressed by the cross section of photon interaction with the substance (as described by e.g. Kolchugkin and Uchaykin, 1978).

Since the detector response $N(E)$ and Δ (the EDR) are determined by the same photon flux, it is obvious that they are functionally related. Assume that this function is determined by the expression:

$$\Delta(\vec{r}_0) = \int_0^{E_0} K(E) N(E) dE \quad (3)$$

Where $K(E)$ is some unknown energy-dependent function. $K(E)$ can be described as $K(E) = \mathbf{j}(\vec{\Omega}^*, \vec{\Omega}) K^*(E)$. Here $\mathbf{j}(\vec{\Omega}^*, \vec{\Omega}_0)$ is the value of the angular detector response function for a fixed aperture $\vec{\Omega}^* \in \Delta\Omega$.

Using (1 - 3), it is easy to show that the function $K(E)$ in equation (3), is the solution to the integral equation:

$$f_a(E') = \mathbf{e}(E') \mathbf{j}(\vec{\Omega}^*, \vec{\Omega}_0) \int_0^{E_0} dE \times K^*(E) \times G(E, E') \quad (4)$$

As equation (4) is linear, the function $K(E)$ may be determined with the accuracy of the constant factor of $\mathbf{j}(\vec{\Omega}^*, \vec{\Omega}_0)$. The integral equation (4) may be solved by the method of Tikhonov *et al.* 1990. The numerical solution of equation (4) for $K^*(E)$ using $\mathbf{j}(\vec{\Omega}^*, \vec{\Omega}_0) = 1$ is shown in Figure 5.4. As mentioned previously, equation (4) is linear, so the function $K(E)$ for $\mathbf{j}(\vec{\Omega}^*, \vec{\Omega}_0) \neq 1$ is related with $K^*(E)$ through the simple relation:

$$K(E) = K^*(E) / \mathbf{j}(\vec{\Omega}^*, \vec{\Omega}_0) \quad (5)$$

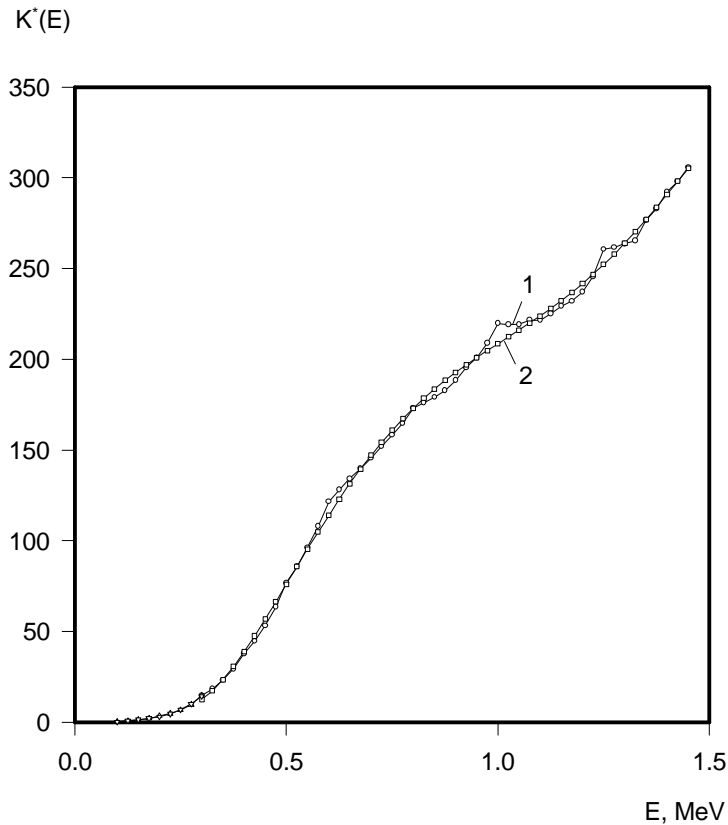


Figure 5.4 $K^*(E)$ versus the photon energy, E . Curve 1 is the numerical solution to equation (4); curve 2 is the approximation of $K^*(E)$ by a fifth order polynomial.

In the following calculations the function $\epsilon(E)$ was approximated by a fifth order polynomial $\epsilon(E) \approx \sum_{i=0}^5 a_i E^i$. This representation of the $\epsilon(E)$ function and the numerical solution to equation (4) are in a good agreement, as can be seen in Figure 5.4.

The detector response function $G(E, E')$ was determined by the Monte-Carlo method, whereas $f_a(E')$ was determined from table values of cross sections for photon interaction with substances (Storm and Israel, 1973). $\epsilon(E')$ is a simple analytical expression for the case of photons perpendicularly incident to the crystal of the scintillator.

The dependence of $\epsilon(E)$ on E , as shown in Figure 5.4, has a simple physical explanation. As mentioned above, the low energy photons have a high detection efficiency, but their contribution to the total dose is smaller than that of the high energy photons with a lower detection efficiency.

The EDR determined according to equation (2) is the contribution to dose from the solid angle $\Delta\Omega$. The total EDR is an additive value and is determined by the formula:

$$D(\vec{r}_0) = \int_{4p} d\vec{\Omega} \int_0^{E_0} dE' f_a(E') \Phi(\vec{r}_0, \vec{\Omega}, E') \quad (6)$$

The surface of the measured objects is replaced by an approximated closed surface consisting of triangles, the corners of each of the triangles being the measuring points. In this case, the integral in expression (6) may be replaced by a sum:

$$D(\vec{r}_0) = \sum_{j=1}^M \Delta P_j(\vec{r}_0) = \sum_{j=1}^M \int_{\Delta\Omega_j} d\vec{\Omega} \int_0^{E_0} dE' f_a(E') \Phi(\vec{r}_0, \vec{\Omega}, E') \quad (7)$$

where $\Delta\Omega_j$ is the solid angle of the j -th triangular surface S_j from point \vec{r}_0 and

$\sum_{j=1}^M \Delta\Omega_j = \int_{4p} d\vec{\Omega}$ is the total number of triangles which cover the whole investigated area.

The photon mean free path in air for practically the whole energy range is several tens of metres (at least for the unscattered radiation), so it is possible to neglect the absorption and reflection in air inside the Sarcophagus. This leads to the expression:

$$\Phi(\vec{r}_0, \vec{\Omega}, E') = \Phi(\vec{r}_s, (\vec{r}_s - \vec{r}_0) / |\vec{r}_0 - \vec{r}_s|, E') \quad (8)$$

expressing that the photon flux is constant along the direction $\vec{\Omega} = (\vec{r}_0 - \vec{r}_s) / |\vec{r}_0 - \vec{r}_s|$ (the point \vec{r}_s lies this direction) when there is no absorption or reflection in the medium.

In this case, the integral in expression (7) along the solid angle $d\vec{\Omega}$ may be replaced by the integral along the triangle surface (see Figure 5.5), using the obvious relation

$$d\vec{\Omega} = \left| \vec{n}_j \vec{\Omega} \right| d\vec{r}_s / |\vec{r}_0 - \vec{r}_s|^2, \quad (9)$$

where \vec{n}_j is a normal to the triangle surface S_j , the point \vec{r}_s is on surface S_j ($d\vec{r}_s \equiv ds$ is an element of the surface area). Equation (9) simply expresses that the solid angle covered by a surface is given by the projected area divided by the squared distance. Thus, taking into account equations (8) and (9), the following can be deduced:

$$\int_{\Delta\Omega_j} d\vec{\Omega} \Phi(\vec{r}_0, \vec{\Omega}, E') = \int_{S_j} d\vec{r}_s / |\vec{r}_0 - \vec{r}_s|^2 \left| \vec{n} \vec{\Omega} \right| \Phi(\vec{r}_s, (\vec{r}_0 - \vec{r}_s) / |\vec{r}_0 - \vec{r}_s|, E') \quad (10)$$

Here $\vec{\Omega} = (\vec{r}_0 - \vec{r}_s) / |\vec{r}_0 - \vec{r}_s|$.

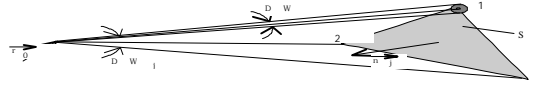


Figure 5.5 The triangle surface element which may be seen from the point \vec{r}_0 under the solid angle $\Delta\Omega_j$.

For the expression (10) the average theorem may be used:

$$\int_{\Delta\Omega_j} d\vec{\Omega} \Phi(\vec{r}_0, \vec{\Omega}, E') = \left| \vec{n} \vec{\Omega}^* \right| \Phi(\vec{r}_0, \vec{\Omega}^*, E') \int_{S_j} d\vec{r}_s / |\vec{r}_0 - \vec{r}_s|^2, \quad \vec{\Omega}^* \in \Delta\Omega_j$$

As the solid angle $\Delta\Omega_j$ is small, the 'average' value $\vec{\Omega}^*$ may be approximated by a arithmetic mean of the three corners of the triangles

$$\int_{\Delta\Omega_j} d\vec{\Omega} \Phi(\vec{r}_0, \vec{\Omega}, E') = \frac{1}{m} \sum_{i=1}^m \left| \vec{n}_j \vec{\Omega}_j \right| \left\{ \frac{1}{\Delta\Omega_j} \int_{\Delta\Omega_j} d\vec{\Omega}_i \Phi(\vec{r}_0, \vec{\Omega}_i, E') \right\} \int_{S_j} d\vec{r}_s / |\vec{r}_0 - \vec{r}_s|^2, \quad m=3. \quad (11)$$

The flux is averaged along the solid angle of the collimator $\Delta\Omega$, here for each direction on the i -th top of a triangle. Thus, using (11), the j -th component of EDR in formula (7) may be represented by:

$$\begin{aligned}
\Delta_j(\vec{r}_0) &= \int_0^{E_0} dE f_a(E) \int_{\Delta\Omega_j} d\vec{\Omega} \Phi(\vec{r}_0, \vec{\Omega}, E) = \\
1/m \sum_{i=1}^m \left| \vec{n}_j \cdot \vec{\Omega}_i \right| & 1/\Delta\Omega \left\{ \int_{\Delta\Omega} d\vec{\Omega}_i \int_0^{E_0} dE f_a(E) \Phi(\vec{r}_0, \vec{\Omega}_i, E) \right\} \int_{S_j} d\vec{r}_s / |\vec{r}_0 - \vec{r}_s|^2 = \\
1/m \sum_{i=1}^m \left| \vec{n}_j \cdot \vec{\Omega}_i \right| & [1/(\langle \vec{j} \cdot (\vec{\Omega}^*, \vec{\Omega}_0) \rangle \Delta\Omega)] \left\{ \int_0^{E_0} K^*(E) N_{ij}(E) dE \right\} \int_{S_j} d\vec{r}_s / |\vec{r}_0 - \vec{r}_s|^2 =
\end{aligned} \tag{12}$$

where $N_{ij}(E)$ is the energy spectrum of the detector for the geometry where it points to the i -th top of the j -th triangle. The function $\eta_j(\vec{r}_0) = \int_{S_j} d\vec{r}_s / |\vec{r}_0 - \vec{r}_s|^2$, corresponds to the substitution of the triangle surface

S_j by a circular surface with the same area and is determined by expression (9).

The expression in square brackets, C_{col} , in expression (12) is the factor of proportionality, which has the following physical meaning: it is the angle seen by the detector through the aperture. This may be found from the apparatus angular function of the collimated detector (see Figure 3.2 and Figure 3.3) or from calibration at the measurement location of the Gamma Locator (i.e. from the value of EDR, (\vec{r}_0)):

$$\begin{aligned}
C_{col} &= [1/(\langle \vec{j} \cdot (\vec{\Omega}^*, \vec{\Omega}_0) \rangle \Delta\Omega)] = \\
(\vec{r}_0) & \left\{ \sum_{j=1}^M \eta_j(\vec{r}_0) 1/m \left(\sum_{i=1}^m \left| \vec{n}_j \cdot \vec{\Omega}_i \right| \left\{ \int_0^{E_0} K^*(E) N_{ij}(E) dE \right\} \right) \right\}
\end{aligned} \tag{13}$$

where M is the number of measurements. For any arbitrary point of the reactor hall, the EDR is described by the formula:

$$(\vec{r}) = C_{col} \left\{ \sum_{j=1}^M \eta_j(\vec{r}) 1/m \left(\sum_{i=1}^m \left| \vec{n}_j \cdot \vec{\Omega}_i \right| \left\{ \int_0^{E_0} K^*(E) N_{ij}(E) dE \right\} \right) \right\} \tag{14}$$

which expresses that changes in the EDR change are taken into account through a geometrical factor, defined by the function $\eta_j(\vec{r})$. This follows from the isotropic angular distribution of flux of the photons, emitted by the surface pseudo-sources of the considered triangles. It is a good approximation for scattered and non-scattered (direct) radiation emitted by contaminated surfaces.

The methodology of the EDR calculation is a reconstruction of the gamma-ray field inside the hall taking into account the energy and angular parameters at the location of the Gamma Locator.

5.2 Calculated Dose Rates inside the Reactor Hall

The calculation of the EDR distribution in the reactor hall was performed according to the algorithm discussed above, using the measurements described in Chapter 4. The EDR calculations were carried out in horizontal sections of planes on a uniform grid with a fixed step size of 1 m. The number of planes

was 36, and the distance in the vertical direction between planes is 1 m. The level of the Gamma Locator was applied as the ‘zero’ horizontal level. In Figure 5.6 and Figure 5.7 the EDR distributions in planes located at levels + 2, + 8 m are shown. The vertical EDR distribution over the centre of the destroyed reactor is shown in Figure 5.8.

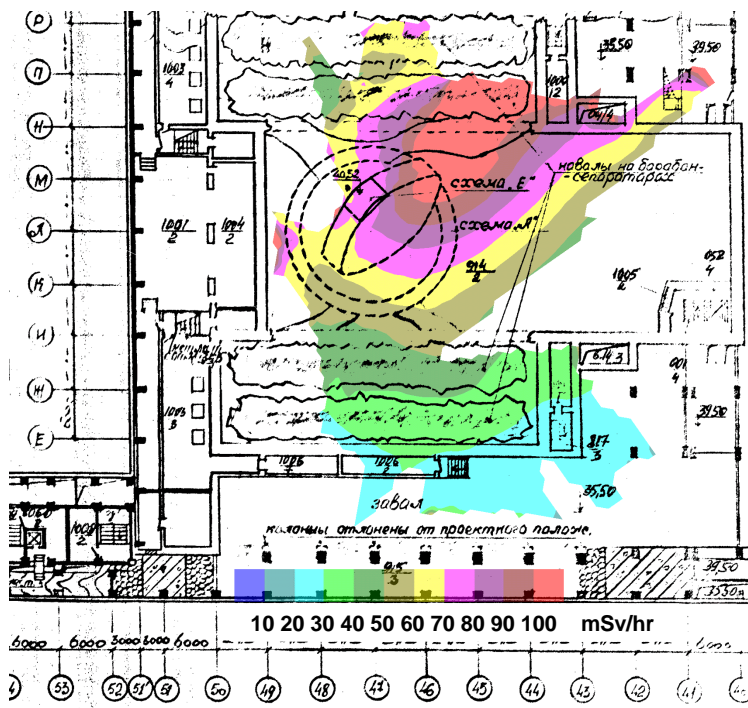


Figure 5.6 The EDR distribution 2 m above the position of the Gamma Locator.

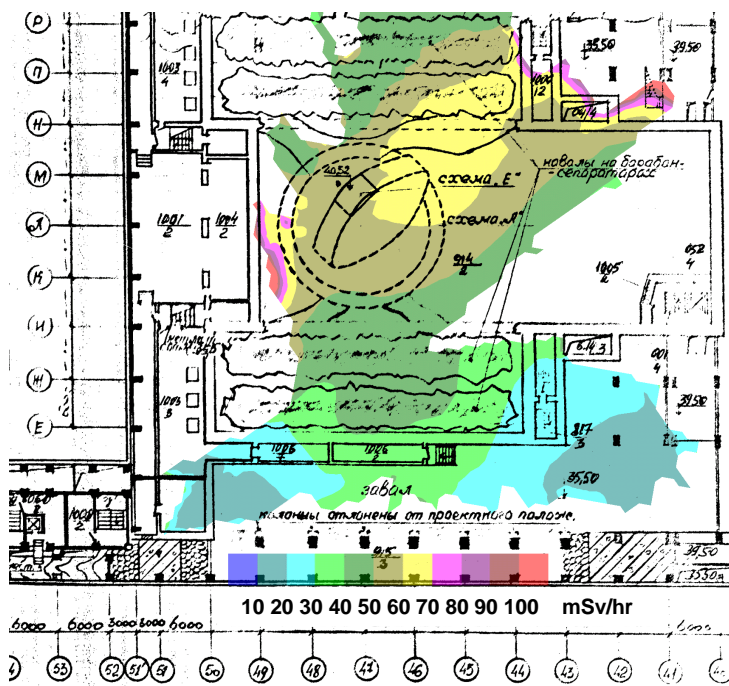


Figure 5.7 The EDR distribution 8 m above the position of the Gamma Locator.

P(h), R/hr

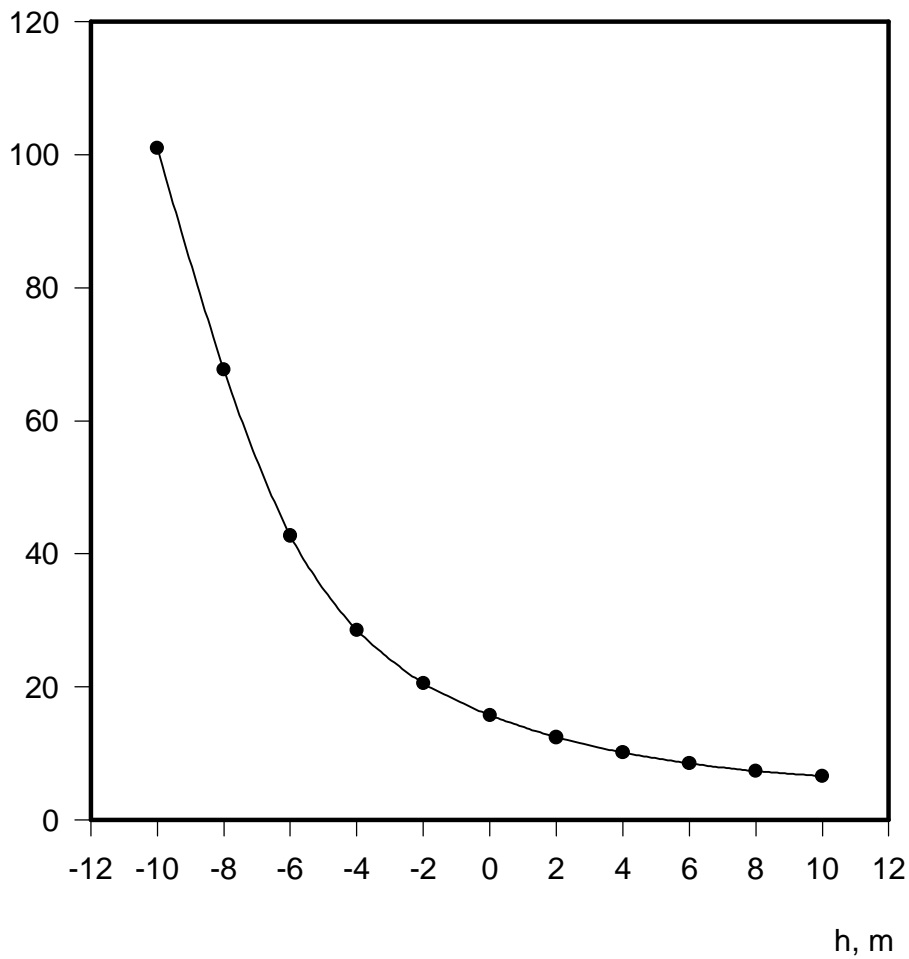


Figure 5.8 Dependence of EDR on the height (at a point near the reactor). The 'EDR equivalent' exposure rate in Röntgens is plotted against the height in metres.

Figure 5.9 shows the results obtained for the EDR in a plane at a level of 8 m above the Gamma Locator, based on surface activities estimated) from the integrated count rate N , b) from the count rate N in range I (400-600 keV),) from the count rate N_f in range II (600-740 keV), d) from the count rate found from the weight function $K()$ (as discussed above).

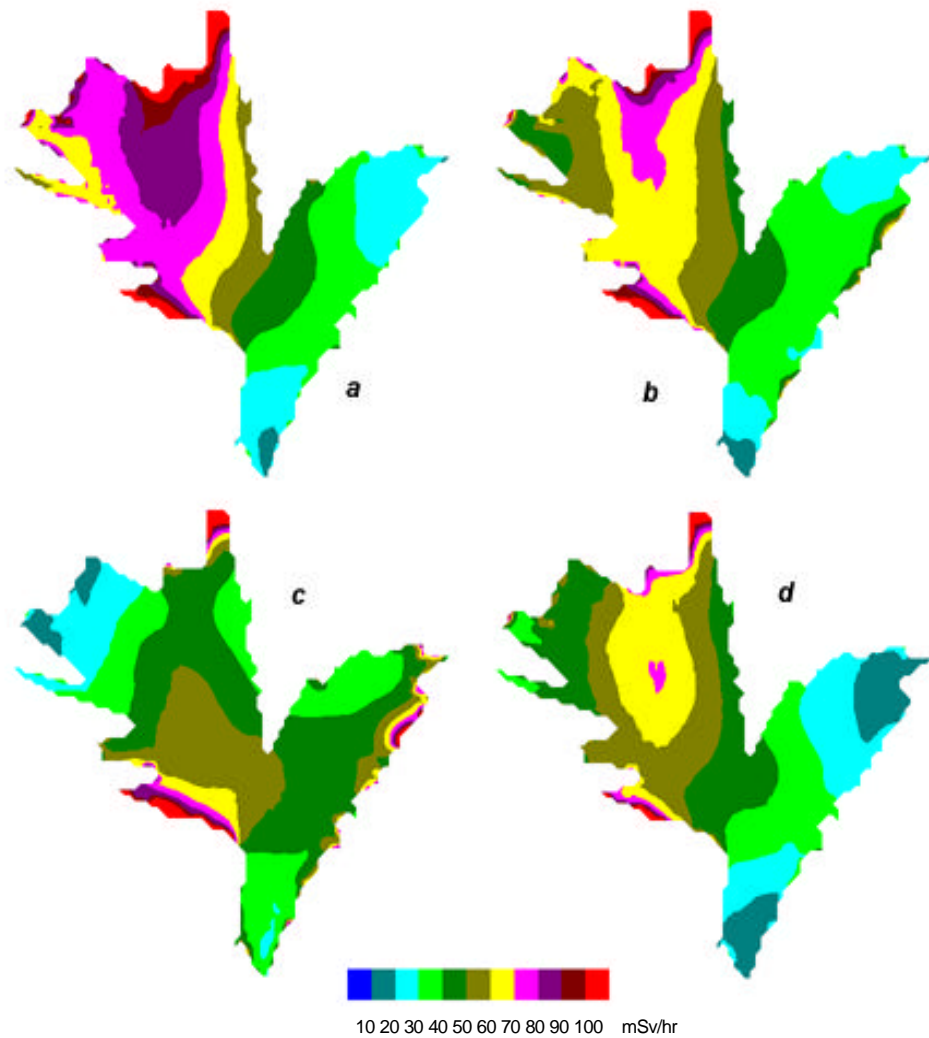


Figure 5.9 EDR Distribution in a plane at a level of 8 m, using an estimation of surface activity based a- on integrated count rate; b - on count rate in range I; c - on count rate in range II; d – on the method of weight function.

The Figure shows, that the pattern of the EDR distribution differs significantly for cases) and). The estimation of EDR based on the integrated count rate is overestimated, and the estimate based on the count rate, N_i , in the photopeak is underestimated. The reasons for the overestimation and underestimation are discussed in section 3.3. The cases b) and d) give the most reliable results and these correspond to each other.

6 Modelling of Forced Dose-Reduction

All the obtained measurement data forms a basis for modelling of implementation of countermeasures to improve the radiation situation. The main objective for the future is to reduce the dose rate inside the building. The main dose contributing sources in the reactor hall are the sources near the destroyed reactor. Since these sources are distributed in volumes, the simplest dose-reductive measure would be to cover them with clean sand, concrete, etc. The dose-reduction simulation was restricted to this procedure only.

To estimate the efficiency of this operation, calculations of the EDR were carried out for the case where a clean layer of sand of 1.7 g/cm^3 in density is applied to cover the reactor area with the angular coordinates ϑ from -12° to -33° and φ from 280° to 327° . From Monte-Carlo calculations it was established, that the influence of the clean layer can be estimated by the change of the effective activity at the surface of the radiation source according to the formula:

$$A^* = A \exp(-\alpha \Delta z),$$

where the factor α is $0.119/\rho$, ρ is the density of the sand [g/cm^3] and Δz (the thickness of the clean sand layer [cm]) is determined from the results of Monte Carlo calculations. The EDR calculations were made in the plane of the CSD arrangement, for thickness of the clean sand layer of $z = 10, 30$ and 50 cm. The results of the calculations of the EDR distribution for $z = 30$ cm are shown in Figure 6.1.

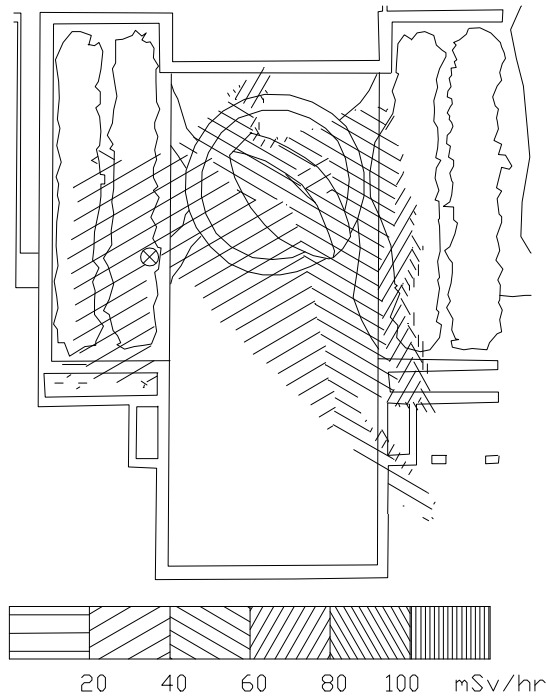
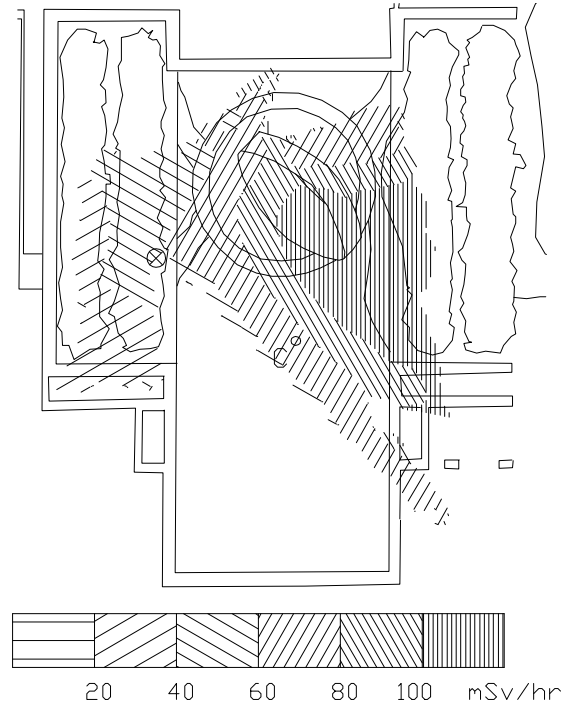


Figure 6.1 The EDR distribution in the reactor hall at the plane of the collimated detector before (top) and after (bottom) decontamination.

To clarify the influence of the clean sand layer, the relative change of the EDR ($\Delta P/P$) at the point indicated with a 'C' in Fig. 6.1 (top) is shown in Fig. 6.2. As can be seen from these Figures, at greater thickness of the layer of sand than z 30-40 cm, the increment in dose reduction is limited, since other radiation sources here give the main contribution to the EDR.

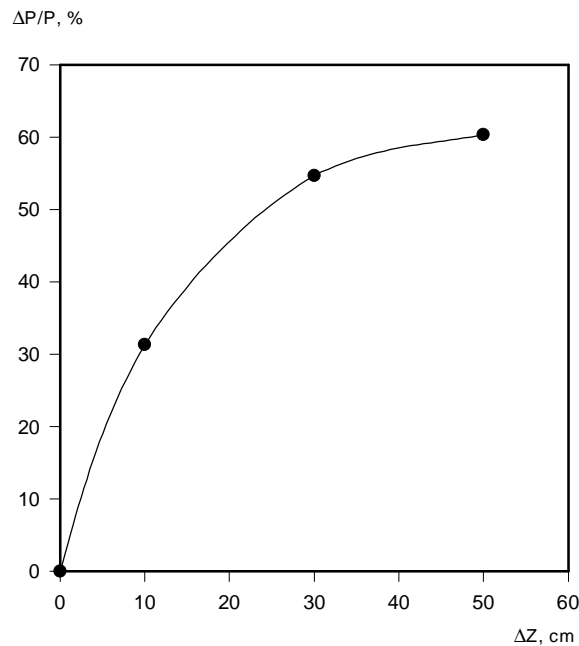


Figure 6.2 The EDR reduction in the reactor hall versus the thickness of the clean sand layer applied

7 Conclusions

The Gamma Locator was developed and tested in the damaged reactor hall of the Chernobyl NPP. The equipment has been used to measure the radiation incident from all angles in the reactor hall. The test showed that it was possible to carry out the complete radiation survey program, although the measuring head was exposed over a three-week period with an exposure rate of as much as 5 R/hr.

From the obtained data, the most intensive sources of gamma radiation were identified. Based on the measurements, the distribution of the surface activity inside the reactor hall was calculated and superposed on maps. The surface activity of the most heavily contaminated places is more than 20 times higher than the average value of the surface contamination. Based on the surface activity distribution, the EDR distribution inside the surveyed building was calculated.

From the measurements it is possible to identify the most efficient ways to reduce the dose rate inside the reactor hall and to estimate the individual contributions to dose rate from the different sources in the building. This type of analysis can be used to form a strategy for further dose reductive action.

The data base generated from the measurements could be supplied with additional data from measurements in other rooms of the 4th unit of the Chernobyl NPP. This would make it possible to establish a computer model of the radiological situation inside and outside the sarcophagus.

8 Acknowledgement

The authors would like to thank Dr. F. Helm (FCK, Karlsruhe, Germany) and Mr. F. Stetner (KHG, Karlsruhe, Germany) for stimulating discussions and help in developing the mathematical model.

This work was partly supported under the framework of the INCO-COPERNICUS program, fixed contribution contract N IC15-CT96-0807 (DG 12-COPE).

9 References

- A.V. Chesnokov, V.I. Fedin, A.P. Govorun et. al., Collimated Detector Technique for Measuring a Cs-137 Deposit in Soil under a Clean Protected Layer, *Appl. Radiat. Isot.* v.48, No 9, pp.1265-1272, 1997b.
- A.V. Chesnokov, S.M. Ignatov, V.N. Potapov et. al., Determination of Surface Activity and Radiation Spectrum Characteristics inside a Building by Gamma Locator, *Nucl. Instr. Meth. A* 401 (1997a) 414-420.
- A.V. Chesnokov, A.A. Gulyaev, S.M. Ignatov et. al. Scanning Remote Gamma-Spectrometer Allowing to Determine Replacement of Radioactive Source, IEEE MIC Conf. Record 1994a , Norfolk, Virginia, USA. Oct.30-Nov.5, 337-340.
- A.V. Chesnokov, A.A. Gulyaev, S.M. Ignatov, et. al. Gamma Locator to Determine Spectrum Characteristics of Quantum Flux, Proc. HSRC/WERC Joint Conference on Environmental, Albuquerque, May 1996, p. 528-536.
- A.V. Chesnokov, V.I. Liksonov S.V. Smirnov, et. al. Radiometry Remote Methods Application at Chernobyl NPP. Conf. Proc. "Spectrum-94", Atlanta, Georgia, USA, August 1994b.
- Z. He, S.V. Guru, D.K. Wehe, et.al.. Portable Wide-Angle γ -ray Vision System. IEEE Trans. on Nucl. Sci. v. 42, No 4, (1995) 647-668.
- O.P. Ivanov, V.N. Potapov, S.B. Shcherbak, L.I. Urutskoev. Calculation of Gamma-Field from Cs-137 Fallout. VI Russian Scientific Conference on Radiation Shielding of Nuclear Installations, Obninsk, September 20-23, Vol. 3, pp. 279-281, 1994.
- A.M. Kolchugkin and V.V. Uchaykin. Introduction in the theory of particles passage through substance. Moscow. Atomizdat, 1978, page 256 (in Russian).
- V.P. Mashkovich. Protection from ionised radiation. Directory, 3-rd issue , Moscow, Energoizdat, 1982 (in Russian).
- G. Mottershead and C.H. Orr. A Gamma Scanner for Pre-decommissioning Monitoring and Waste Segregation. *The Nuclear Engineer*, v. 37, No 1, (1996), 3-7.
- G. Simonet. Remote Gamma-ray Mapping: ALADIN Nuclear Installation Remote Activity Locating Device, in CEC Topical Meeting on Non-destructive Assay of Radioactive Waste, Cadarashe, France (1990).

- E. Storm and H. Israel. Cross Section of interaction of gamma-rays (for energy of 0.0001-100 MeV and elements of number 1 to 100). Directory. Moscow. Atomizdat, 1973, page 256 (in Russian).
- A.N. Sudarkin, O.P. Ivanov, V.E. Stepanov, A.G. Volkovich, A.S. Turin, A.S. Danilovich, D.D. Rybakov, L.I. Urutskoev. High-energy radiation visualizer (HERV): A new system for imaging in X-ray and gamma-ray emission regions, IEEE Trans. NS-43, No.4, (1996) 2427-2433.
- A.N. Tikhonov, A.V. Goncharski, V.V. Stepanov, A.T. Aygola. Numerical methods of the decision incorrect tasks, Moscow, Science, 1990 page 187 (in Russian).
- A.V. Volkovich, V.I. Liksonov, et. al. Application of Collimated Detector for Removal of accident consequence in machine room in 4-th Unit of ChNPP., Atomic energy, v. 69, No 6, (1990) 389-391 (in Russian).
- A.V. Volkovich, V.I. Liksonov, et. al. Measurements of Distribution of Surface Activity in Reactor Shaft of 4-th Unit of ChNPP., Atomic energy, v. 69, No 3, (1990), 164-170 (in Russian).

Title and authors

Surface Activity Distribution Measurements and Establishment of a Dose Rate Map inside the Destroyed Chernobyl Reactor

A.V. Chesnokov, V.I. Fedin, A.A. Gulyaev, V.N. Potapov, S.V. Smirnov, S.B. Shcherbak, L.I. Urutskoev, A.G. Volkovich, H. Würz, C.L. Fogh, K.G. Andersson, J. Roed

ISBN		ISSN	
87-550-2444-0; 87-550-2445-9 (Internet)		0106-2840	
Department or group		Date	
Nuclear Safety Research and Facilities Department		February 1999	
Groups own reg. number(s)		Project/contract No(s)	
		NIC15CT960807	
Pages	Tables	Illustrations	References
42	1	28	16

Abstract (max. 2000 characters)

A Gamma Locator designed for contamination survey inside the reactor hall of the 4th unit of Chernobyl NNP has been developed. The device consists of a detector head and a remote control computer connected by a 150 m long cable. The detector head (dimensions: 500mm by 500mm by 400mm; weight: about 40 kg) is a collimated scintillation gamma detector (the collimation angle is 10°). It is installed on a scanning unit and was placed inside the reactor hall. The Gamma Locator scans all surfaces of the reactor hall with angular steps ($\geq 1^\circ$ vertically as well as horizontally) and the particle fluence from the corresponding direction is recorded. The distance between the device head and the measured surface is instantaneously registered by a laser distance gauge. Inside the collimator there is a small CCD camera which makes it possible to obtain a visible image of the measured surface. The effective surface activity levels are presented in colour on the screen of the control computer. The gamma detector essentially consists of a CsI(Tl) scintillator crystal ($\varnothing 8$ mm in diameter, 2.5 mm in thickness) and a Si photodiode. The detector energy resolution is about 8% for radiation from ^{137}Cs . The exposure dose rate distribution in the reactor hall is estimated from the measured effective surface activities (^{137}Cs is the main gamma emitting isotope inside the reactor hall). The results of dose rate calculations are presented in colour superposed on a drawing of the reactor hall.

Descriptors INIS/EDB

CESIUM-137; CHERNOBYLSK-4 REACTOR; DOSE RATES; GAMMA DETECTION; MAPPING; REACTOR ACCIDENTS; SCINTILLATION COUNTERS; SURFACE CONTAMINATION

Available on request from Information Service Department, Risø National Laboratory.

(Afdelingen for Informationsservice, Forskningscenter Risø), P.O.Box 49, DK-4000 Roskilde, Denmark.

Telephone +45 46 77 40 04, Telefax +45 46 77 40 13